NAVAL POSTGRADUATE SCHOOL

MONTEREY, CALIFORNIA

THESIS

OBSERVED STATISTICS OF EXTREME WAVES

by

Anne Marie Laird

December 2006

Thesis Advisor:	Thomas H. C. Herbers
Second Reader:	Edward B. Thornton

Approved for public release; distribution is unlimited

THIS PAGE INTENTIONALLY LEFT BLANK

REPORT DOCUMENTATION PAGE		Form Approved OMB No. 0704-0188

1. AGENCY USE ONLY *(Leave blank)*	2. REPORT DATE December 2006	3. REPORT TYPE AND DATES COVERED Master's Thesis

4. TITLE AND SUBTITLE Observed Statistics of Extreme Waves	5. FUNDING NUMBERS
6. AUTHOR Anne Marie Laird	
7. PERFORMING ORGANIZATION NAME AND ADDRESS Naval Postgraduate School Monterey, CA 93943-5000	8. PERFORMING ORGANIZATION REPORT NUMBER
9. SPONSORING /MONITORING AGENCY NAME AND ADDRESS N/A	10. SPONSORING/MONITORING AGENCY REPORT NUMBER

11. SUPPLEMENTARY NOTES The views expressed in this thesis are those of the author and do not reflect the official policy or position of the Department of Defense or the U.S. Government.

12a. DISTRIBUTION / AVAILABILITY STATEMENT Approved for public release; distribution is unlimited.	12b. DISTRIBUTION CODE A

13. ABSTRACT

Amphibious landings and small boat operations are normally conducted only in benign wave conditions. An unexpected encounter with an isolated freak wave may damage equipment and prevent mission accomplishment. This study examines the occurrence of unusually large waves using data sets obtained with bottom mounted pressure sensors and wave buoys in the DUCK 94, SHOWEX, and SAX 04 experiments. All of the experiments include wave records from high energy events. After correcting the raw pressure data for hydrodynamic attenuation over the water column, the statistics of wave heights were evaluated and compared with the theoretical Rayleigh distribution of a narrow-band linear wave field.

Observations from deep water sites follow the Rayleigh distribution well, even in extreme sea states, indicating that strong nonlinearity does not have a major effect on wave height statistics. However, during high energy events at shallow water sites, there are significantly less measured wave heights in the right-hand tail of the distribution of wave heights than the theoretical Rayleigh distribution would predict. These results show that waves become more homogeneous in height as they propagate into shallower water, possibly owing to breaking and nonlinear effects. While the observed wave statistics do not suggest a frequent occurrence of freak waves, isolated large waves were indeed observed, even in benign conditions. Further studies are needed to assess their risk to Navy operations.

14. SUBJECT TERMS Undersea Warfare, Freak Waves, Sea State, Ocean Waves, SAX 04, DUCK 94, SHOWEX, Nonlinear, Wave Buoys, Pressure Sensors, Histogram	15. NUMBER OF PAGES 67
	16. PRICE CODE

17. SECURITY CLASSIFICATION OF REPORT	18. SECURITY CLASSIFICATION OF THIS PAGE	19. SECURITY CLASSIFICATION OF ABSTRACT	20. LIMITATION OF ABSTRACT
Unclassified	Unclassified	Unclassified	UL

NSN 7540-01-280-5500

Standard Form 298 (Rev. 2-89)
Prescribed by ANSI Std. 239-18

THIS PAGE INTENTIONALLY LEFT BLANK

Approved for public release; distribution is unlimited

OBSERVED STATISTICS OF EXTREME WAVES

Anne M. Laird
Lieutenant, United States Navy
B.S., United States Naval Academy, 2000

Submitted in partial fulfillment of the
requirements for the degree of

MASTER OF SCIENCE IN PHYSICAL OCEANOGRAPHY

from the

NAVAL POSTGRADUATE SCHOOL
December 2006

Author: Anne Marie Laird

Approved by: Thomas H. C. Herbers
Thesis Advisor

Edward B. Thornton
Second Reader

Mary L. Batteen
Chair, Department of Oceanography

Donald P. Brutzman
Chair, Undersea Warfare

THIS PAGE INTENTIONALLY LEFT BLANK

ABSTRACT

Amphibious landings and small boat operations are normally conducted only in benign wave conditions. An unexpected encounter with an isolated freak wave may damage equipment and prevent mission accomplishment. This study examines the occurrence of unusually large waves using data sets obtained with bottom mounted pressure sensors and wave buoys in the DUCK 94, SHOWEX, and SAX 04 experiments. All of the experiments include wave records from high energy events. After correcting the raw pressure data for hydrodynamic attenuation over the water column, the statistics of wave heights were evaluated and compared with the theoretical Rayleigh distribution of a narrow-band linear wave field.

Observations from deep water sites follow the Rayleigh distribution well, even in extreme sea states, indicating that strong nonlinearity does not have a major effect on wave height statistics. However, during high energy events at shallow water sites, there are significantly less measured wave heights in the right-hand tail of the distribution of wave heights than the theoretical Rayleigh distribution would predict. These results show that waves become more homogeneous in height as they propagate into shallower water, possibly owing to breaking and nonlinear effects. While the observed wave statistics do not suggest a frequent occurrence of freak waves, isolated large waves were indeed observed, even in benign conditions. Further studies are needed to assess their risk to Navy operations.

THIS PAGE INTENTIONALLY LEFT BLANK

TABLE OF CONTENTS

THIS PAGE INTENTIONALLY LEFT BLANK

LIST OF FIGURES

LIST OF TABLES

THIS PAGE INTENTIONALLY LEFT BLANK

ACKNOWLEDGMENTS

Heartfelt gratitude is extended to my advisor, Dr. Thomas H.C. Herbers, for his guidance, patience, and instruction during my pursuit of this research. I am also grateful for Mr. Paul Jessen, for providing dedicated technical help. His assistance in MATLAB programming and creating the structure for several figures in this thesis is greatly appreciated.

I want to express my gratitude to my family, particularly to my husband, Robert, especially since he had his own thesis and TSSE project to complete in the Mechanical Engineering curriculum. I am also grateful for my beautiful daughter Clara (USNA Class of 2027 hopeful) for making me realize that come 1600 everyday, I should be playing with her instead of further refining my MATLAB code.

THIS PAGE INTENTIONALLY LEFT BLANK

I. INTRODUCTION

A. HISTORICAL BACKGROUND

Extreme waves have been a part of mariner folklore for centuries. Sailors speak of walls of water, or of holes in the sea, which appear without warning. Until approximately 20 years ago, such reports were dismissed as fanciful sea stories, about as credible as sightings of leviathans and mermaids. As early as 1826, Captain Dumont d'Urville, a French scientist and naval officer in command of an expedition, reported encountering waves 80 to 100 feet high. He was openly ridiculed for making such an outrageous report, even though three of his colleagues supported his estimate (Draper, 1964).

The world's oceans claim on average one ship a week, often in mysterious circumstances. But with little evidence to draw from, investigators usually attribute these losses to human error or a ship's poor maintenance record. However, an alarming series of disappearances and near-sinkings, including world-class vessels with unblemished safety records, has prompted the search for a different cause and a renewed belief in a maritime myth: the so-called freak wave.

These suspicions were reinforced in 1978 by the loss of the München, a state-of-the-art cargo ship (Rosenthal, 2006). The storms predicted when she set out to cross the Atlantic did not concern her seasoned German crew. The voyage was perfectly routine until at 0300 on 12 December, she sent out a garbled mayday call from North of the Azores. Rescue attempts began with over a hundred ships combing the area; the ship was never found. An exhaustive search found just a few bits of wreckage, including an un-launched lifeboat that bore a vital clue. It had been stowed 20 meters above the water line yet one of its attachment pins had twisted as though it was hit by an extreme force.

B. FIRST RELIABLE DATA OF EXTREME WAVES

Since these extreme waves are so rare, a problem arises obtaining a sufficient sample size for research. An experienced mariner might only experience one of these extreme waves in a lifetime . . . if he survives it. In February 1933, the United States Navy steamship Ramapo ploughed into a Pacific storm en route to Manila, Philippines, from San Diego. The wind blew at an unremitting 60 knots for seven days, producing 15

meter swells. On the morning of 7 February, an extreme wave came from behind the ship, first tossing her into a deep trough, then lifting her stern-first over the wave crest. As the stern of the 146 meter ship reached the bottom of the trough, the officer on watch triangulated the wave against the ship's crow's nest. The 34 meter estimated wave height – about as tall as an 11-story building (Draper, 1971) – remains the biggest wave ever reliably measured.

One of the British Ocean Weather Ships, operating in all types of weather conditions in the North Atlantic, carried one of the first data recording devices that could reliably measure wave heights. As the ship was on station for about two-thirds of the time, the British National Institute of Oceanography obtained a long series of wave records which were taken for fifteen minutes every three hours. At first the scale of the instrument could record waves 50 feet high from crest to trough, but very soon it was found that waves higher than this were not uncommon and the scale was increased to 60 feet. This scale proved sufficient for about nine years, but on September 12, 1961, 'Weather Reporter' was navigating on a course that lay close to the track of the dying Hurricane Betsy, and as she made her routine recording at 0900 the pen dipped and touched the lower edge of the chart and then rose rapidly and 'hit the stops' at the top of the grid. A crest was fitted to this wave and it is estimated that the true height of the wave was not less than 67 feet from crest to trough (Figure 1). The probability that the 'Weather Reporter' actually recorded the highest wave which hit the vessel is fairly small, because their instrument was only operated about eight percent of the time while the vessel was underway. At the time, the wave which 'Weather Reporter' measured was the highest one ever recorded by an instrument (Draper, 1964).

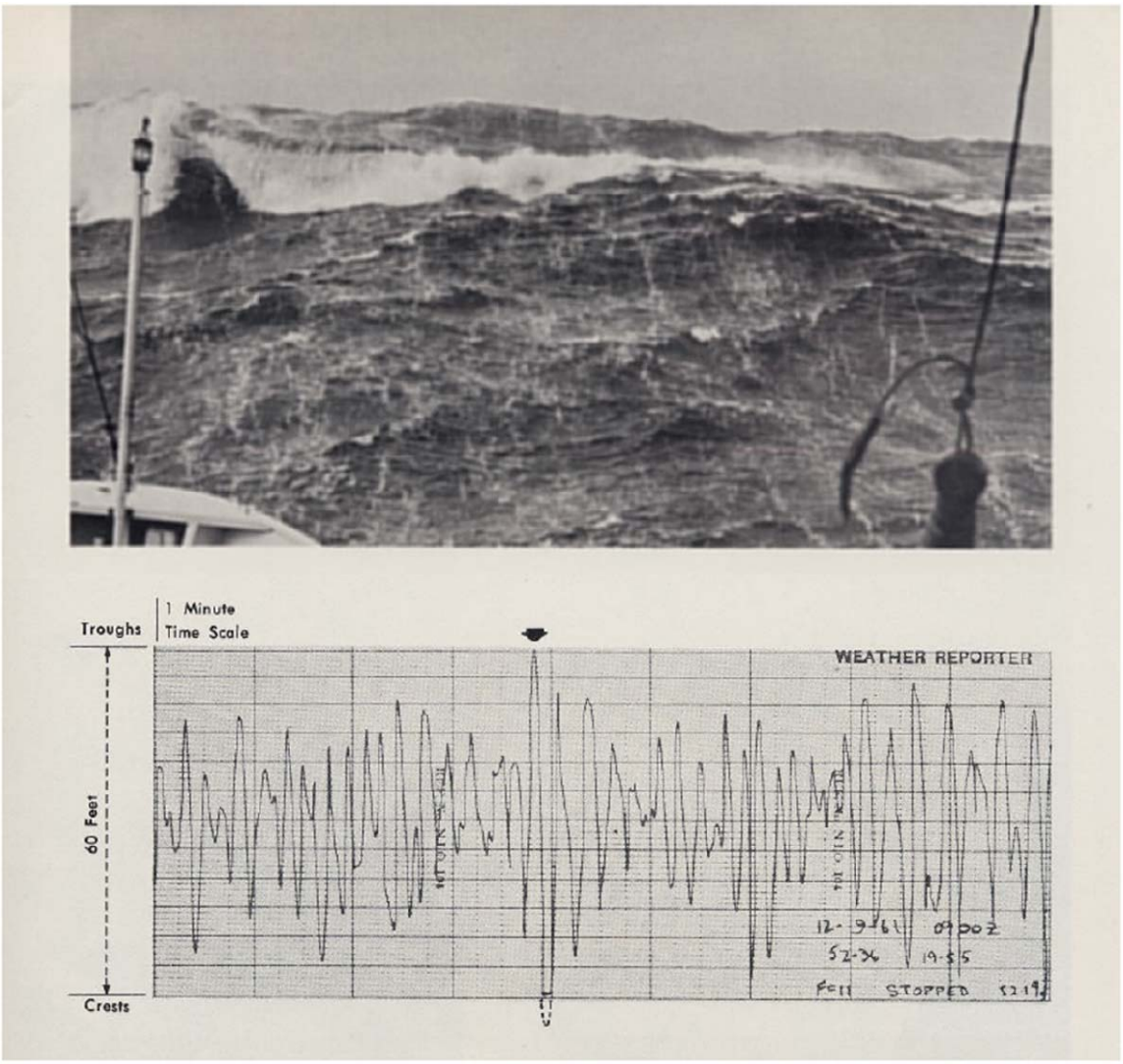

Figure 1. Wave Height time series recorded by the British Ocean Weather Ship 'Weather Reporter.' (From: Draper, 1964)

C. THE "NEW YEAR WAVE" – THE DRAUPNER PLATFORM

The most spectacular sighting in recent years is what has been known in the international scientific community as the "New Year Wave," which hit Statoil's Draupner gas platform in the North Sea on New Year's Day 1995. The significant wave height – the average height of the one-third highest waves – at the time was around 12 meters. In the middle of the afternoon the platform was struck by something much bigger. According to measurements made by a downward-looking laser altimeter, the wave was 26 meters from trough to crest (Haver, 2000a). The maximal amplitude of 18.5 meters (Figure 2) was more than three times the significant amplitude for the wave train, and the maximal

wave height was more than twice the significant wave height (Dysthe et al., 2006). An isolated large wave like this – exceeding twice the significant wave height – is classified as an extreme wave (Lawton, 2001).

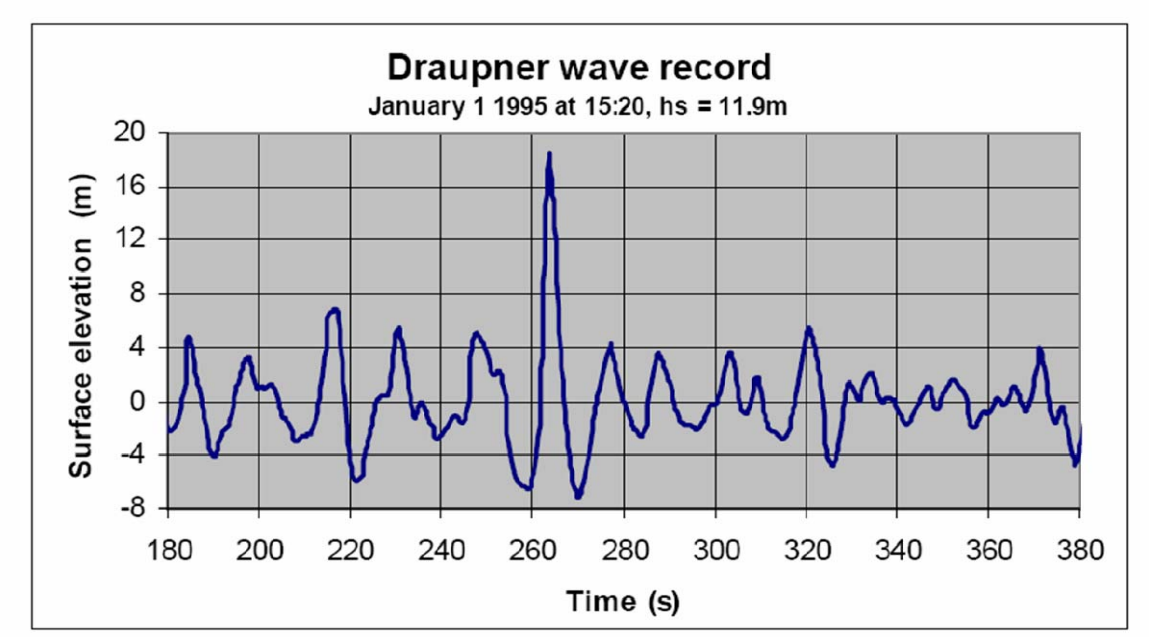

Figure 2. Surface elevation time series of extreme wave event recorded at Draupner oil platform. (From: Haver, 2000a)

D. THEORIES REGARDING EXTREME WAVE FORMATION

The phenomenon of extreme waves is still a matter of active research, so it is too early to state with certainty what the most common causes of formation are, or whether surrounding bathymetry and ambient currents play a role. Until recently, oceanographers assumed that they formed in a straightforward, linear process. According to this view, large waves are simply the product of constructive interference in a linear superposition of many small waves (Dysthe et al., 2006).

One theory to explain large wave formation emphasizes the interaction between a current and an opposing wind field. The phenomenon of wind-current interaction is certainly prevalent in some locales. The waters off Cape Agulhas, the southernmost tip of Africa where the Atlantic and Indian Oceans meet, are a good example of this. Vessels rounding the cape are regularly hit with unusually large waves generated when the fast-flowing Agulhas current collides with westerly winds blowing in from the Southern

Ocean. As wind-generated waves propagate into the current, they steepen and increase in height. Other extreme wave hotspots, notably the Gulf Stream, the Kuroshio current south of Japan and the seas off Cape Horn, also have the fast currents and countervailing winds that produce large waves.

Another theory of large wave formation is current focusing. Even though the current velocities in the open ocean, far from coastal areas, are small (typically about 10 cm/s) they can cause gradual refraction of waves over long distances. The result can be local focusing and diffraction of wave energy. White and Fornberg (1998) have proposed this as an explanation of extreme wave formation. Figure 3 shows wave trajectories through an area of variable current. The current field is faintly marked in the background. It can be seen that all wave trajectories are parallel initially. The deflection due to the current produces areas of both increased and decreased wave intensity.

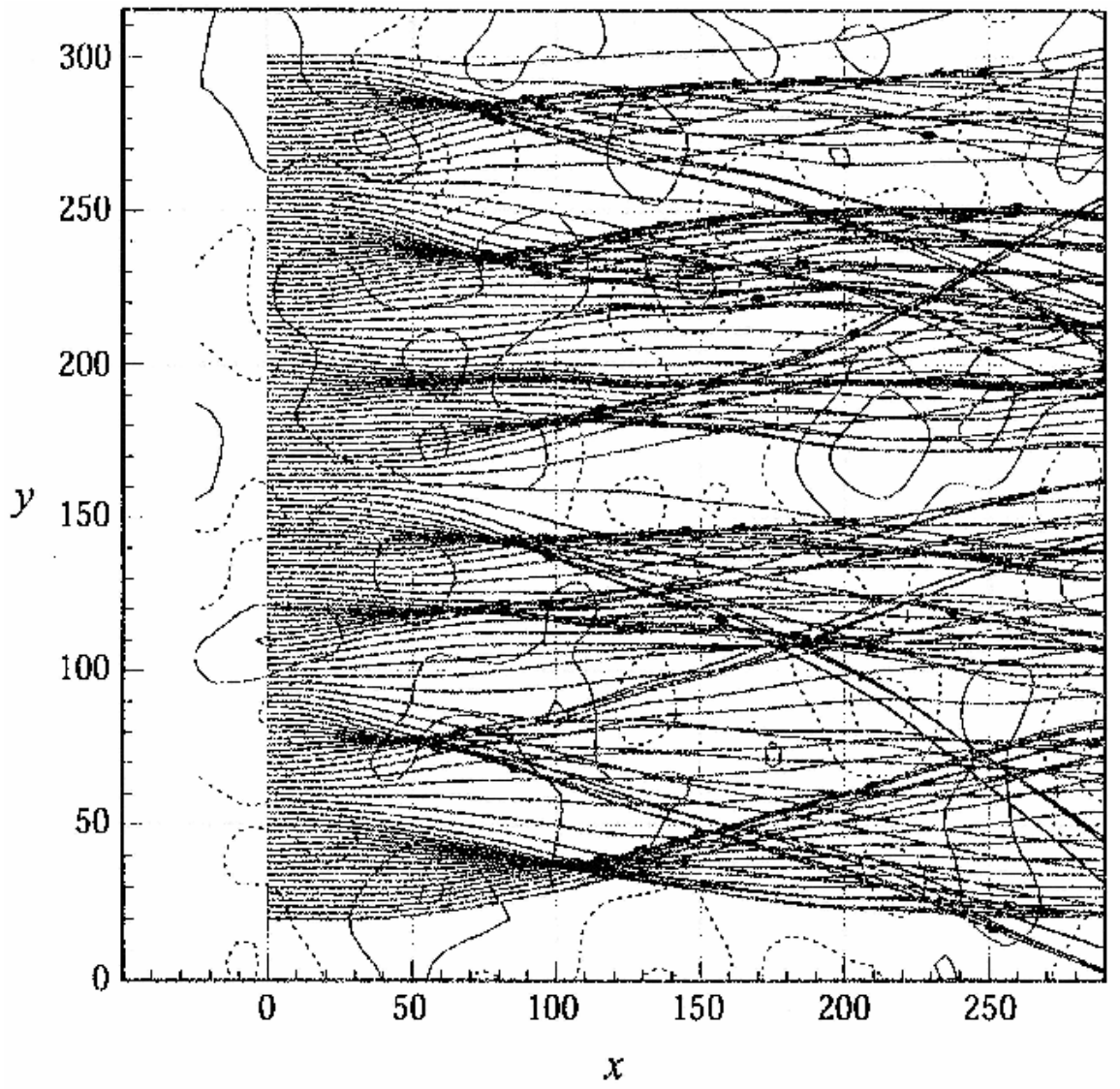

Figure 3. Areas of increased and decreased wave intensity due to wave trajectories traveling through an area of variable current. (From: White et al., 1998)

There are several problems with invoking these mechanisms to explain all extreme waves. First, they do not account for the large number of extreme waves in places such as the North Sea where there are no fast-flowing currents. Secondly, in order for the current focusing model to work, the waves are required to enter the zone of variable currents with a single direction; this assumption is obviously invalid in the real ocean. Thirdly, the wind-current interactions seem to increase heights of all waves, rather than causing isolated large ones. Even where wind-current interference does occur, extreme waves should not be so common. Interference effects ought to produce a normal

distribution of wave heights with the vast majority close to the average height. Outliers to this distribution can occur, but they should occur rarely. It is still an open question whether freak waves are outliers that should be expected or simply 'unusually large' waves.

In December 2000, the European Union initiated MaxWave, a scientific project whose goals were to confirm the widespread occurrence of extreme waves, model how they occur, and consider their implications for ship and offshore structure design criteria. As part of MaxWave, radar data from the European Space Agency's (ESA) satellites were first used to carry out a global extreme wave census. ESA's twin spacecraft ERS-1 and 2 – launched in July 1991 and April 1995 respectively – both have Synthetic Aperture Radar (SAR) as their main instrument. The SAR worked in several different modes; while over the ocean it worked in wave mode, acquiring 10 by 5 kilometer 'imagettes' of the sea surface every 200 kilometers. The ESA provided the researchers with three weeks worth of data; around 30,000 separate imagettes. Despite the relatively brief length of time the data covered, the MaxWave team identified more than ten individual extreme waves around the globe above 25 meters (82 feet) in height (Haver, 2000b). Faced with observations that standard linear theory can not explain, oceanographers and mathematicians are currently examining the effect that nonlinearity has on wave behavior.

Many systems, from the weather to financial markets can follow nonlinear patterns which create outlandish swings in behavior. Tiny changes in initial behavior can have disproportionate consequences. Oceanographers reasoned that the same may be true of the ocean; just with small changes in wave height, speed or direction, extreme waves may be produced. To explore this possibility, researchers have started experimenting with nonlinear mathematical models to see if they produce extreme behavior in ocean waves.

Osborne et al., (2000) used the Nonlinear Schrödinger (NLS) Equation to simulate the evolution of groups of waves. Though originally developed to describe the quantum behavior of electrons in an atom, it has since been applied to various types of waves and predicted their evolution in space and time. Osborne's predictions show that in

certain unstable conditions, waves can steal energy from their neighbors. Adjacent waves shrink while the one at the focus can grow to an enormous size.

Dysthe (2000) has shown that nonlinear interaction between four colliding waves can produce extreme wave behavior. He utilized the NLS equation in his numerical simulations which contained waves colliding in deep water. Other researchers use different equations to model the nonlinear behavior. Pelinovsky et al., (2000) demonstrated the formation of extreme waves using the Korteweg de Vries (KdV) equation, which is valid in shallow water.

It was shown in the mid-1960s that if uniform periodic waves are generated at one end of a long wave tank, the waves will spontaneously split into groups, which get more prominent as they propagate along the tank. According to linear theory these waves should remain uniform and periodic (Figure 4). A modified form of the NLS equation predicts nonlinear wave group development similar to that observed in laboratory experiments. (Trulsen et al., 2001)

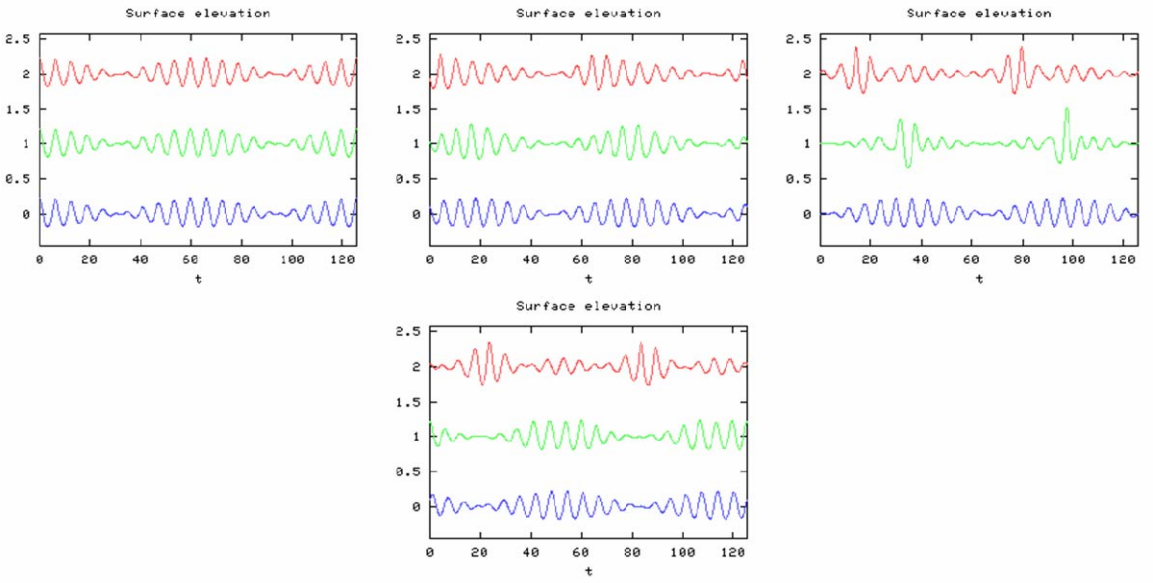

Figure 4. Time series at four stations in a numerical wave tank. The lower (blue) curve shows linear evolution. The middle (green) curve shows evolution according to the NLS equation. The upper (red) curve shows the evolution according to a higher order modified NLS equation. (From: Dysthe et al., 2006)

Even the simplest NLS equation has an exact solution that evolves into isolated freak waves. It starts out as a periodic wave train where the amplitude is weakly modulated. After some time it develops a particularly strong focusing of wave energy by which a small part of the wave train "steals" energy to build itself up at the expense of the amplitudes of the surrounding waves (Figure 5).

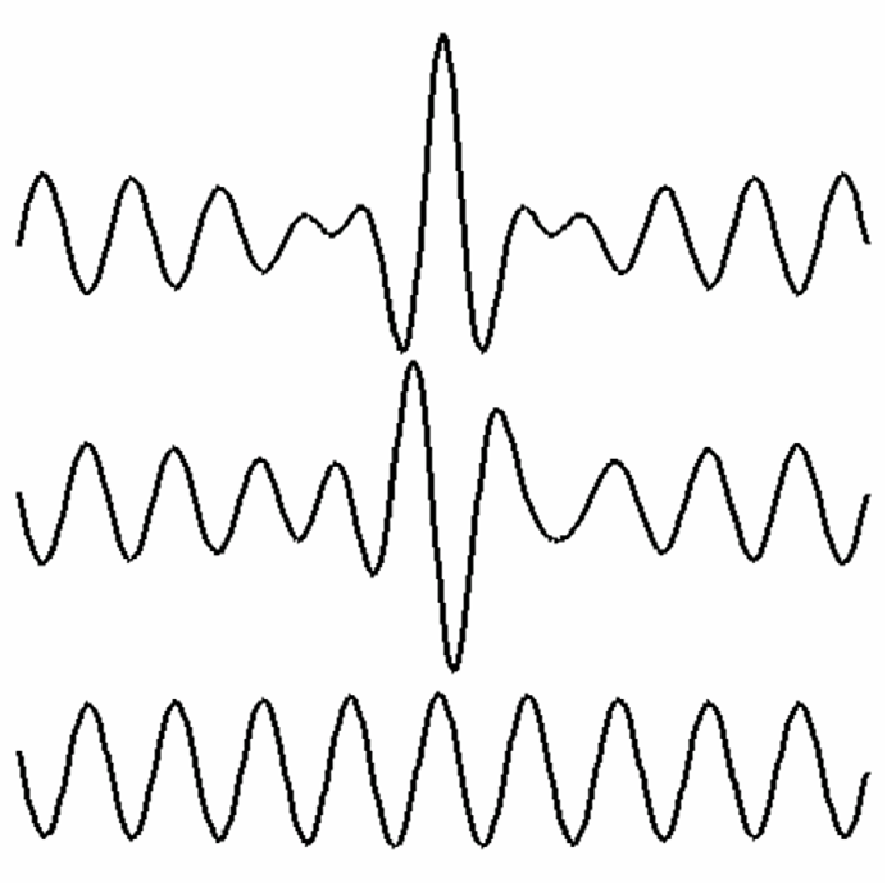

Figure 5. An energy stealing wave as a solution to the NLS equation. (From: Dysthe and Trulsen, 1999)

Although this nonlinear process provides a possible explanation for freak waves in the ocean, the narrow band approximation in NLS type equations is violated in most natural sea states and the nonlinear evolution of realistic broadband wave fields is still poorly understood. They also do not explain the diversity in the reports of extreme wave sightings, ranging from walls of water that are spotted on the radar long before they come into view, to steep crests that appear from nowhere and disappear just as quickly. Some nonlinear models produce groups of three, four or even five huge waves in a row, giving credibility to the feared "three sisters" – three massive waves in quick succession. "When the seas get steep, you get a lot of nonlinearity," says oceanographer Linwood Vincent of the U.S. Office of Naval Research. (Lawton, 2001)

E. CONTROVERSY SURROUNDING EXTREME WAVE RESEARCH

A main source of controversy is the question whether extreme waves are a statistical anomaly. Some researchers claim that if wave height records are collected over a significant length of time, they will fit a smooth probability distribution with the vast majority of the wave heights close to the average height, and the unusually large waves are simply the expected waves you will get once in a while to fill in the right-tail of the distribution. Other researchers reject this idea, claiming that the presence of extreme waves cannot be explained with statistical models. Instead they propose dynamical mechanisms for the generation of unusually large waves (i.e., that exceed twice the significant wave height) involving strong nonlinearity, and suggest that these extreme waves appear more often then predicted by a statistical distribution.

A major difficulty in modeling highly nonlinear waves is the computational effort involved in simulating two-dimensional sea surfaces. Both the frequently used NLS and KdV equations are one-dimensional models, which assume unidirectional wave propagation. Currently, researchers are developing models which are two-dimensional, but so far no comprehensive results have been published regarding the formation of extreme waves.

F. LINEAR WAVE THEORY AND THE RAYLEIGH DISTRIBUTION

To gain a better understanding of the nature of freak waves, it is useful to first examine the statistics of linear models with observed wave data before making a departure into the effects of nonlinearity. In linear theory, there are no freak waves present. The sea surface is described as a linear superposition of many statistically independent sinusoidal wave components (Figure 6) with different frequencies, which travel in different directions. Applying the central limit theorem, it follows that the sea surface height obeys a Gaussian (i.e., normal) distribution. Thus in a linear model, obtaining a sea surface height measurement that exceeds four standard deviations would occur with a very small probability of 0.01267%.

One important characteristic of linear wave fields is their group structure. For example, consider two waves with the same amplitude, and slightly different frequencies that travel in the same direction. Using the principle of superposition, the resulting sea surface displacement may be written as:

$$y(t) = y_m \sin\left(\left(\omega + \Delta\omega\right)t\right) + y_m \sin\left(\left(\omega - \Delta\omega\right)t\right)$$

$$= 2y_m \cos(\Delta\omega t)\sin(\omega t)$$

which represents a sinusoidal oscillation with frequency ω that is modulated at the difference frequency $\Delta\omega$. Thus the interference of the two waves results in a variation of the amplitude (bottom panel of Figure 6) that explains the beat pattern of wave groups.

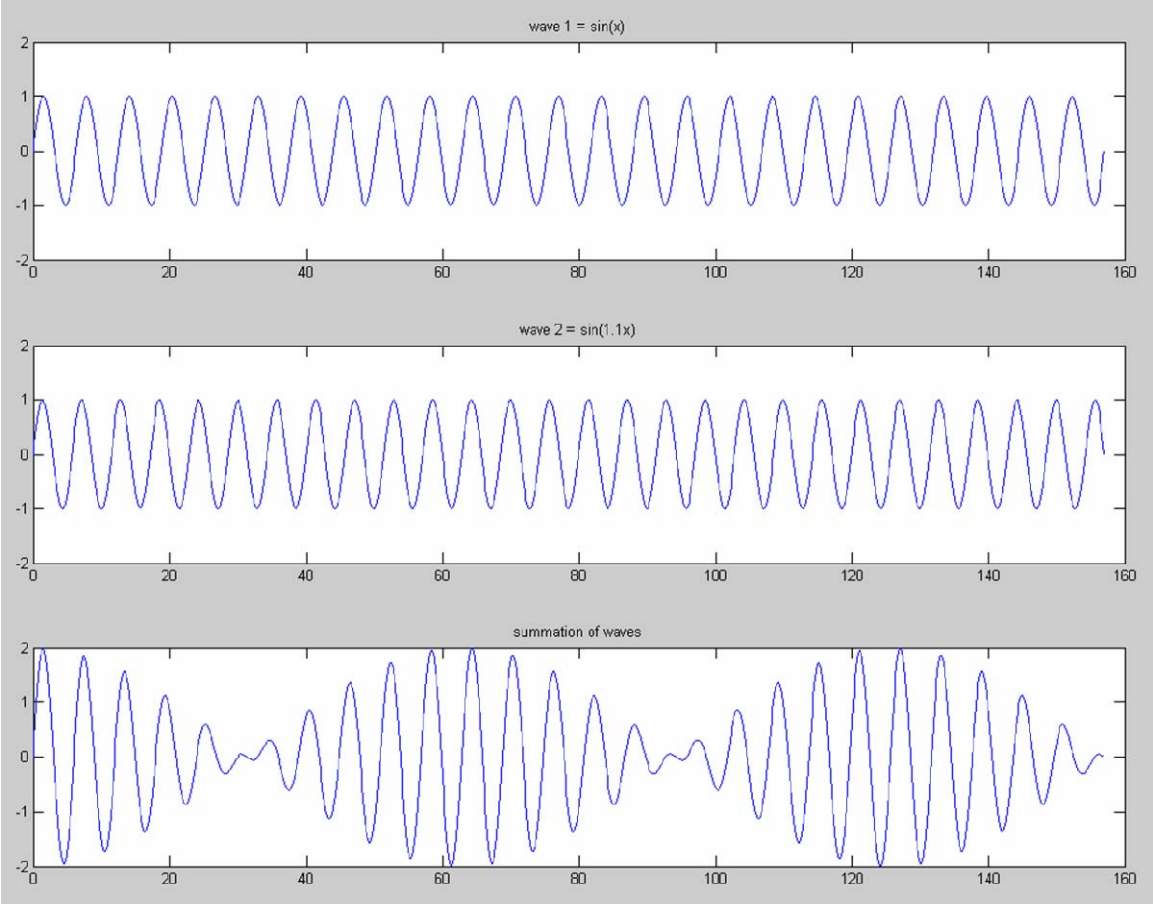

Figure 6. The summation of two sinusoidal waves with slightly different wavelengths produces the wave groups shown in the bottom panel.

In the linear models, the statistics of wave heights can be quantitatively described by the Rayleigh probability distribution (Longuet-Higgins, 1952). For the Rayleigh distribution to be valid, the waves must be linear and narrow banded in both frequency and direction. That is, the wave field can be characterized with an average frequency $\overline{f}$, and a mean direction $\overline{\theta}$.

The Rayleigh wave height probability density function (pdf) is

$$p(H) = \frac{2H}{H_{rms}{}^2} \exp\left[-\left(\frac{H}{H_{rms}} \right)^2 \right]$$

This equation is completely specified by H_{rms}, the root mean square wave height. Although this distribution is not expected to be valid in broad wind-generated seas or in

very shallow water (where nonlinear effects are strong), field data show that the Rayleigh model is surprisingly robust, and can be applied to a much wider range of conditions than the strict assumptions of a narrow band, linear process would imply. In fact, Thornton and Guza (1983) found that even well within a surf zone wave height data are reasonably well described by the Rayleigh distribution (Figure 7).

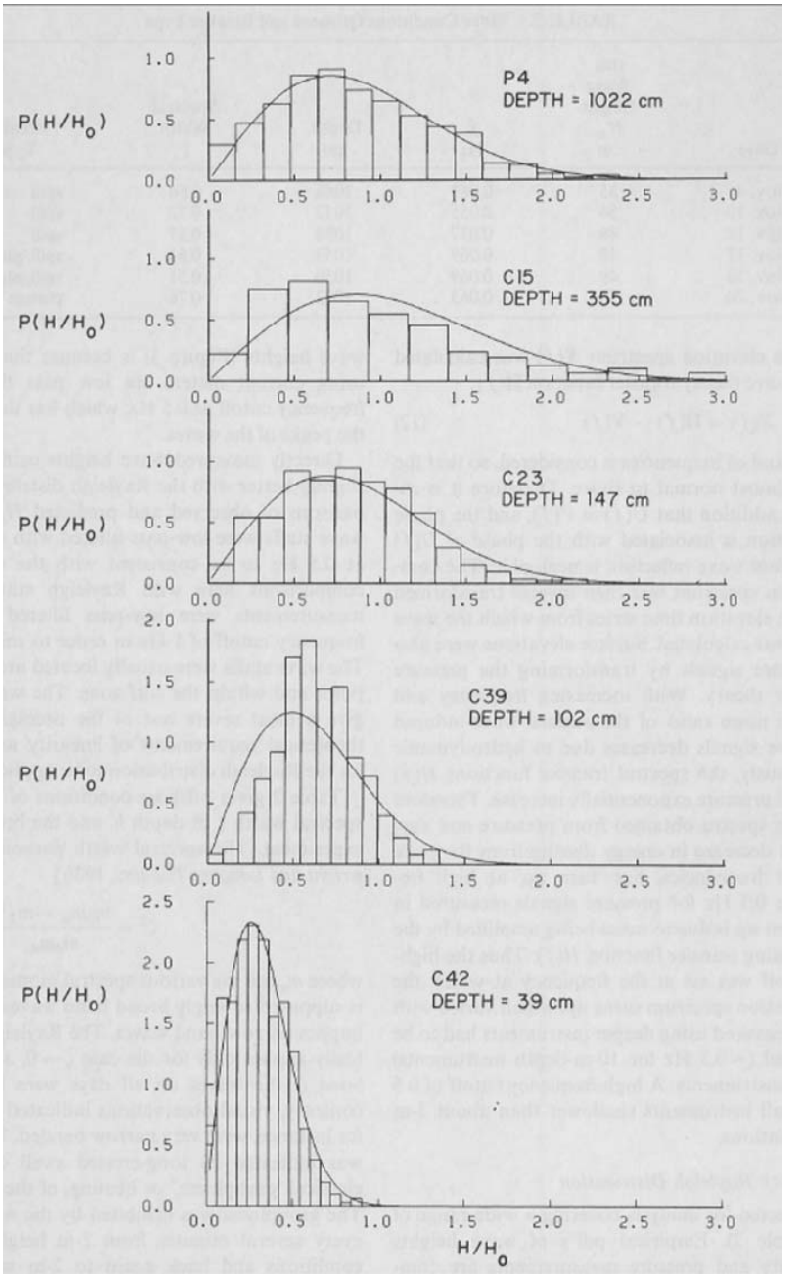

Figure 7. Empirical probability density functions observed on a California beach on November 20, 1978 are compared with the Rayleigh pdf. H_o is H_{rms} in ~10 m depth = 0.5 m (From: Thornton and Guza, 1983).

G. SCOPE OF THIS STUDY

This thesis examines data from several experiments in coastal areas that are unaffected by strong currents but are affected by nonlinearity to examine its importance to the observed statistics of wave heights and the occurrence of freak waves. Previous observations of freak waves were mostly limited to deep water regions; very little is known about the characteristics of these waves in coastal areas. This study compares statistics from energetic wave fields across several depths of water to better understand the nature of these extreme waves as they propagate toward coastal waters. The primary objective of this study is to contribute to the base of knowledge that is needed for safe conduct of naval operations in coastal areas including small boat operations and amphibious operations.

THIS PAGE INTENTIONALLY LEFT BLANK

II. DATA SETS

This study examines data sets obtained with bottom mounted pressure sensors and surface-following buoys in the Office of Naval Research (ONR) sponsored DUCK 94, SHOWEX, and SAX 04 experiments. All of the experiments include time periods when hurricanes or storms approached or passed through the data collection areas. The data sets are described in this chapter.

A. DUCK 94

The first set of field data used in this study was collected as part of the DUCK 94 Nearshore Processes Experiment conducted offshore of the U.S. Army Corps of Engineers Field Research Facility (FRF) near Duck, North Carolina, between late July and early December 1994. The coast consists of a series of relatively straight barrier islands with sandy beaches that are exposed to the Atlantic Ocean. The continental shelf is 50-100 km wide and 20-50 m deep. An array of battery-powered internally recording bottom pressure sensors were deployed along a cross-shelf transect extending from the Duck beach to the shelf break (Figure 8).

Only the two shallowest sensors from the array were used in this study. The shallowest instrument located at Site X, was mounted on a pipe jetted into the beach in 6 m depth just outside the surf zone. The other instrument at Site A, was mounted inside the anchor of a surface mooring at a depth of 12 m. The sensor at Site A was 1 km seaward of the sensor at Site X (Figure 8). Pressure data were recorded nearly continuously with a 2 Hz sample rate (Herbers et al., 2000). At site A, a malfunctioning data acquisition system was replaced in the middle of the experiment with a cassette tape data storage system that utilized a reduced sampling scheme (a 137 minute record sampled at 1 Hz every 3 hours). Both sensors failed during Hurricane Gordon on November 17, when they were buried by sand. For a more detailed description of the DUCK 94 field data, the reader is referred to Herbers et al., (2000).

B. SHOWEX

The second set of field data used in this study was collected as part of the Shoaling Waves Experiment (SHOWEX); extensive wave measurements were collected from September to December 1999. The experiment was conducted in the same general

location as the DUCK 94 experiment. The continental shelf is smooth and relatively featureless and the wave refraction effects are mild in this area (Ardhuin et al., 2003).

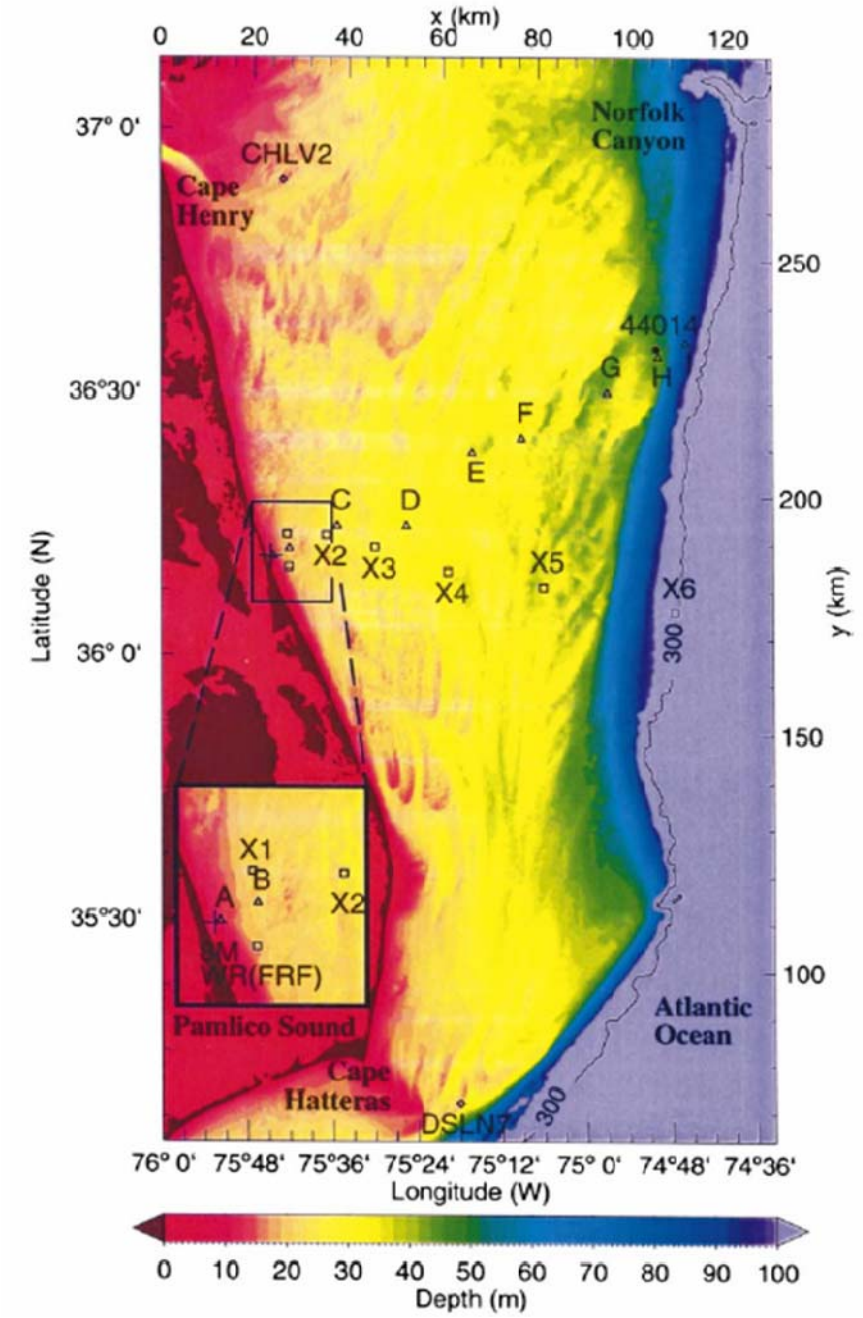

Figure 8. Bathymetry and instrument locations during DUCK 94 and SHOWEX, see Table 1 for instrument locations. Site X from DUCK 94 is approximately 1 km inshore of Site A. (From: Ardhuin et al., 2003)

A transect of six surface-following Datawell Directional Waverider Buoys (X1 – X6) was deployed extending almost due east from the Duck beach to the shelf break. Only the data obtained from Buoys X1 and X6 were utilized in this study. Buoy X6 broke loose on September 21, was redeployed on October 15, and lost again from December 5 through the end of the experiment. Buoy X1 was operational throughout the experiment.

The buoy located closest to shore (X1) transmitted its data via an HF radio link to a receiver mounted on a 50 m high tower at the FRF, while the other buoy (X6), which was out of HF range, used an internal data logger. For a more in-depth description of the SHOWEX field experiment and the associated hardware used, the reader is referred to Tinder (2000) and Ardhuin et al., (2003).

SHOWEX took place during a particularly active hurricane season (Figure 9). Within two days of instrument installation, Hurricane Floyd made landfall south of Cape Hatteras. The maximum offshore significant wave height was 9 m at X6 with a peak frequency of 0.11 Hz. Immediately after Floyd dissipated, a new hurricane, Gert, reached Category 4, but remained far offshore, sending large amplitude swell over the continental shelf (3 m significant wave height at X6). These two major hurricanes were followed by two weaker hurricanes. The eye of Hurricane Irene crossed the Florida Peninsula from the Gulf of Mexico into the Atlantic and passed 100 km offshore of Cape Hatteras, while Jose followed a track similar to that of Gert. SHOWEX was also marked by several nor'easter storms, with a particularly strong storm passing through the region on 1 December.

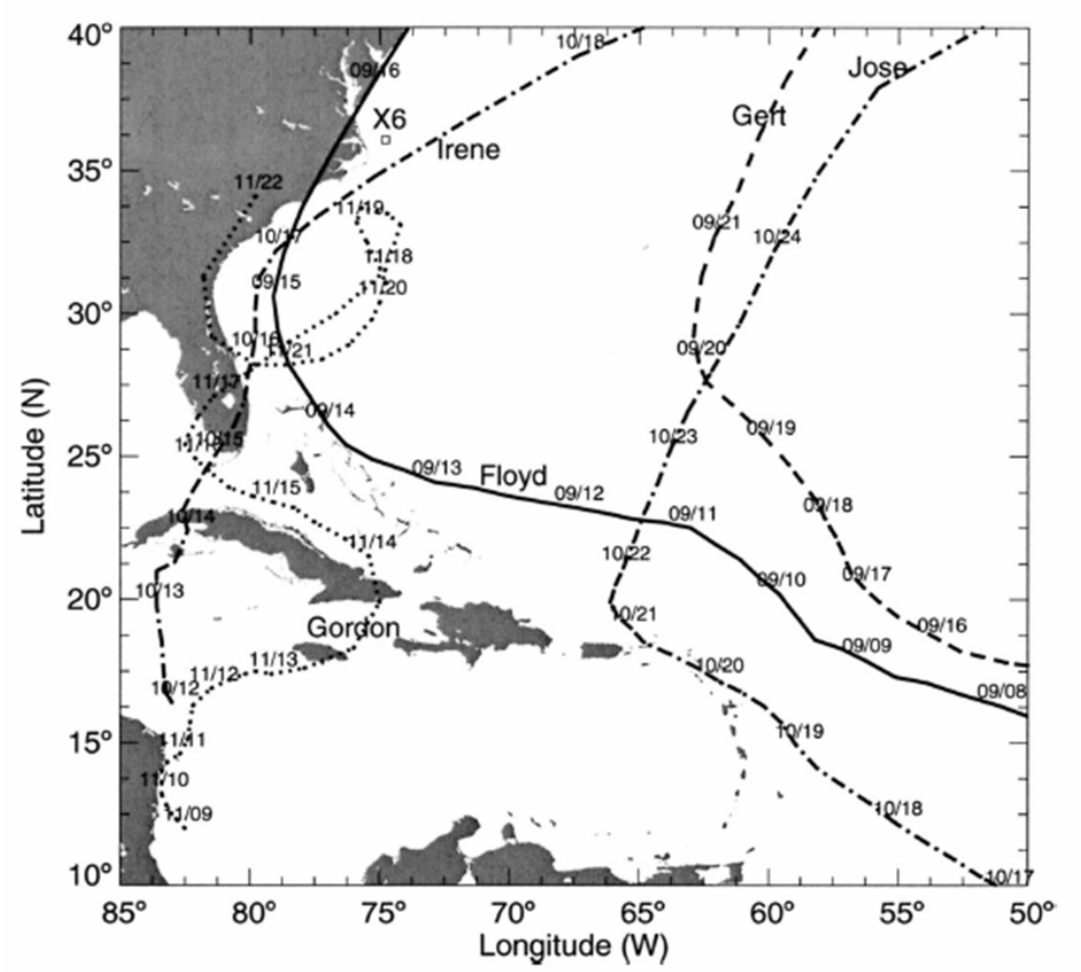

Figure 9. Tracks of North Atlantic Hurricanes Gordon (during DUCK 94), Floyd, Gert, Irene, and Jose (all four during SHOWEX). The dates indicate the daily position of the eye of the storm, at 1200 EST, after reaching the tropical depression stage. The easternmost buoy in SHOWEX (X6) is also indicated. (From: Ardhuin et al., 2003)

C. SAX 04

The third set of field data used in this study was collected as part of the SAX 04 experiment, which was aimed at understanding acoustic propagation through sediments. The experiment was conducted off Panama City, Florida from early September through the middle of November of 2004. To support the intensive acoustic/geological studies, a suite of wave measurements was collected by the Naval Postgraduate School (Figure 10). Bottom pressure data were collected at six sites: 3-7 and 9. Instrument platforms at sites 1, 2 and 8 were lost in the extreme wave conditions of Hurricane Ivan. This study primarily utilizes three sites, 3, 4 and 9, that were in depths of 20 m or less and exposed

to energetic hurricane waves $(H_{rms} > 2\,m)$. Details of the SAX 04 wave measurements and analyses of the observed extreme hurricane generated waves are given in Fernandes (2005).

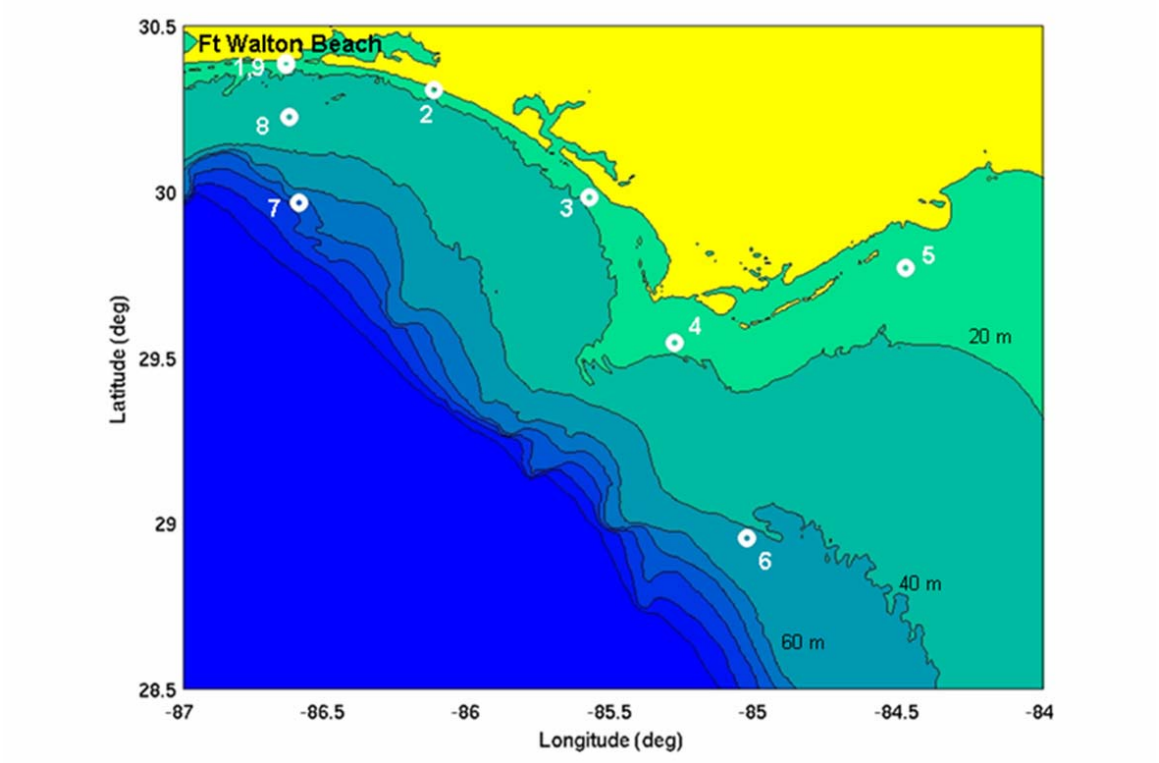

Figure 10. Geographical location of the nine deployment sites in SAX 04. Contours indicate the continental shelf bathymetry at 20 m intervals.

Table 1. Geographical location, depth and sensor type for the seven sensors used from the three ONR sponsored experiments.

Experiment	Site Identifier	Latitude (N)	Longitude (W)	Depth (m)	Sensor Type
DUCK 94	X	36° 12.00'	75° 42.00'	6	pressure
DUCK 94	A	36° 11.40'	75° 44.24'	12	pressure
SHOWEX	X1	36° 13.62'	75° 42.28'	21	buoy
SHOWEX	X6	36° 04.98'	75° 47.47'	195	buoy
SAX 04	3	29° 59.01'	85° 34.99'	17	pressure
SAX 04	4	29° 32.11'	85° 17.24'	15	pressure
SAX 04	9	30° 22.91'	86° 38.37'	18	pressure

THIS PAGE INTENTIONALLY LEFT BLANK

III. DATA ANALYSIS

A. RAW DATA TO SEA SURFACE HEIGHT

Whereas the surface following buoys provide direct measurements of sea surface elevation, the pressure sensors on the sea floor measure an attenuated wave signal. A linear theory depth correction was applied to convert the pressure time series to a sea surface elevation time series. The pressure data were processed in overlapping segments containing 8,192 data points each (approximately one hour). A Fast Fourier Transform was performed on each segment of data. Next, a frequency-dependent correction was applied to the Fourier amplitudes to account for attenuation of the pressure signal between the surface of the water and the sensor on the seabed. In the linear approximation, this attenuation factor is $\frac{\cosh kD}{\cosh kH}$, where D is the height of the sensor above the sea bed, and H is the total water depth. The wavenumber k is given by the dispersion relation $\omega^2 = gk \tanh kH$, where ω is the wave frequency and g is gravity. Inherent in this correction is a limitation at high frequencies. When the sensor depth H-D exceeds the surface wavelength, the weak wave pressure signal is usually not detectable in the background noise, and useable sea surface data cannot be extracted. Due to this limitation, this study only uses data from sensors in water depths of 20 m or less.

After the pressure correction was successfully applied, an Inverse Fast Fourier Transform was performed to obtain a sea surface height time series for each segment of 8,192 data points. To eliminate the "ringing" effect of spectral leakage, the overlapping segments were combined, discarding the overlapping 512 data points on either end of the segment. In this way the hourly surface height files could be merged in a single continuous time series for the entire instrument deployment.

B. ZERO-DOWN CROSSING ANALYSIS

To analyze the statistics of individual waves, the 'zero down crossing method' was applied to the sea surface time series (Figure 11). In this method, wave height is defined as the difference of the maximum and minimum occurring between two consecutive zero down crossings. The wave period is the time (seconds) between successive zero down crossings. The results using this method with an input of sea surface height obtained via a

pressure sensor are very sensitive to the definition of mean level about which the zero down crossings are computed. If the mean of the entire deployment were to be used, errors would be introduced into the data associated with tides and storm surges. To define an appropriate mean water level over a shorter time scale of a group of waves, a five minute average sea level was used. This procedure was not applied to the buoys, which have an internal high pass filter at 0.03 Hz that removes any low-frequency sea level variability.

Demeaning the data is a three step process. First, a five minute average of the data is computed. Second, the five minute average is interpolated back to the raw 2 Hz data. Finally, the interpolated data is subtracted from the raw sea surface height data. The demeaned surface elevation data were then subjected to the zero-crossing analysis to determine wave heights and periods of individual waves.

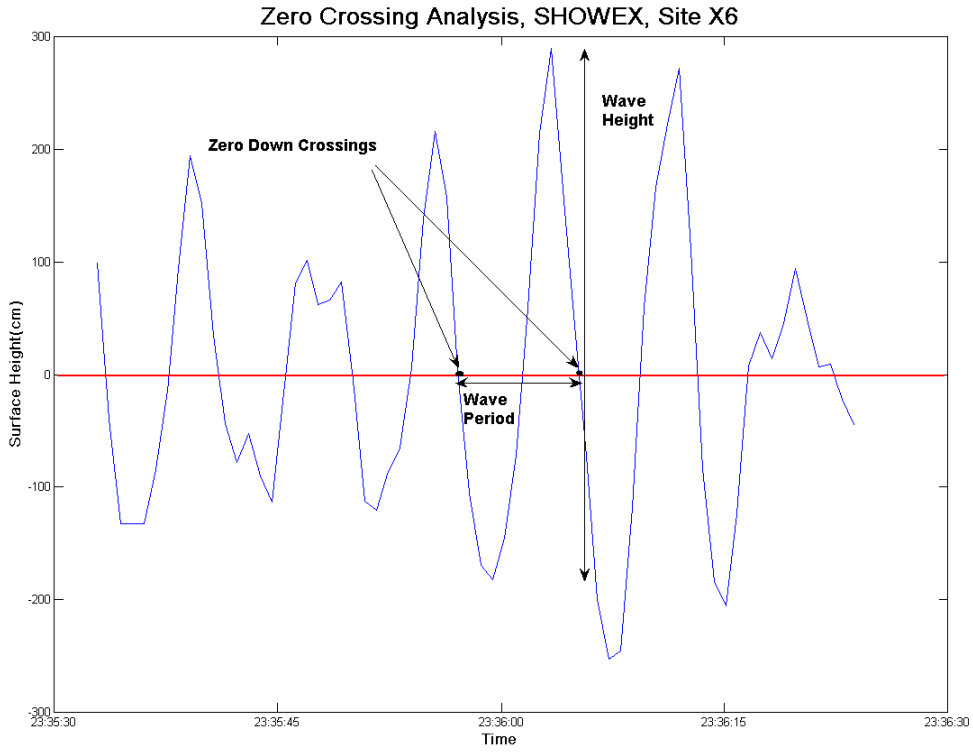

Figure 11. Analysis utilizing zero down crossing method.

C. HISTOGRAMS

The primary focus of this study is wave height statistics, which are examined using histograms of wave heights from one-hour segments of sea surface data. A histogram of wave height distribution was created for each hour of data collected. These histograms will be compared with the theoretical Rayleigh pdf for a linear narrowband wave field. Of particular interest is the question whether nonlinear wave-wave interactions in high sea states have a significant effect on the distribution of wave heights.

The histogram bin width was chosen to be constant for ease of comparing results at different sites. The choice of this bin width represents a tradeoff between having enough data in each bin for a stable estimate of the associated probability and enough resolution to resolve the probability density function. After some trial and error, an appropriate bin width of the distribution of normalized $\left(\frac{H}{H_{rms}}\right)$ wave heights was determined to be 0.1.

For each hour-long record, the wave height data were normalized by dividing by the root mean square wave height from that hour. The relative frequency counts were normalized by the bin width so that the total area under the histogram is equal to 1. This normalization in both the x and y axes allowed comparison between histograms from different experiments and comparison to analytical probability density functions. An example histogram is shown in Figure 12 to agree well with the theoretical Rayleigh pdf.

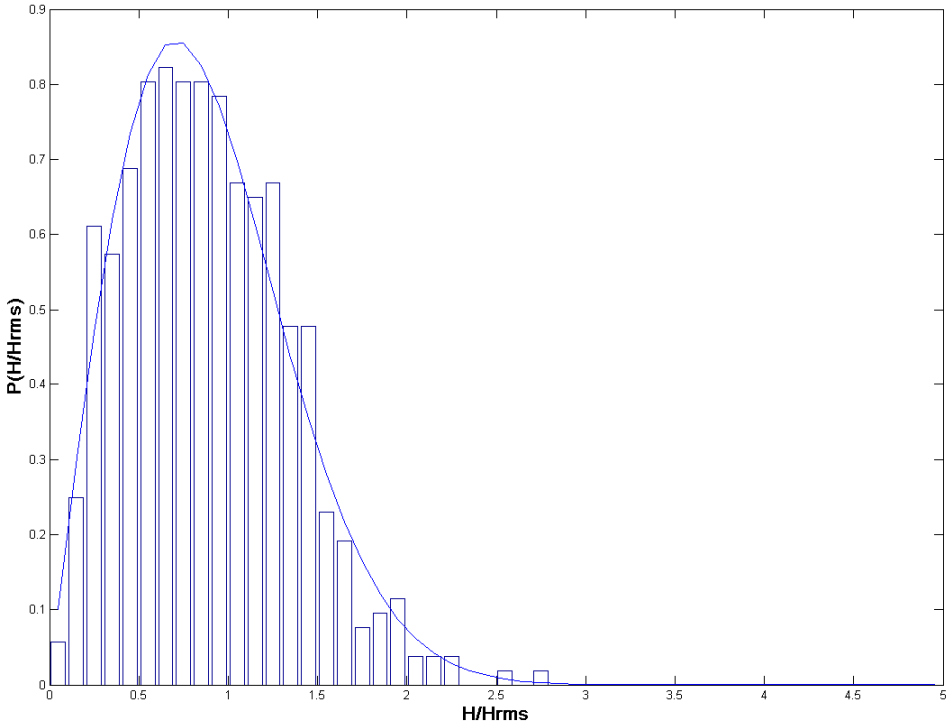

Figure 12. An example histogram generated from 1 hour of sea surface elevation data from the DUCK 94 experiment with a Rayleigh pdf superimposed.

IV. WAVE HEIGHT OBSERVATIONS

A. WAVE HEIGHT STATISTICS

1. Overall Wave Conditions

Before examining the dependence of wave height statistics on sea state, it is useful to give an overview of wave conditions and statistics for all three experiments used in this thesis. The DUCK 94 and SHOWEX experiments took place in the Atlantic Ocean, on the eastern seaboard off of North Carolina, while SAX 04 was conducted in the Gulf of Mexico. The wave climate in the Gulf of Mexico is relatively benign, with the exception of an occasional hurricane, and thus the wave heights observed in SAX 04 under normal conditions were much lower than those observed in the DUCK 94 or SHOWEX experiments. If there was not a hurricane passing through the area of experimentation, the rms wave heights collected in the SAX 04 experiment were well below 1 m. Comparatively, it was relatively common during low energy sea states in SHOWEX and DUCK 94 for the rms wave heights to measure between 1 m and 1.5 m. The most energetic events during the experiments were a Nor'easter in mid-October and Hurricane Gordon during DUCK 94, Hurricanes Floyd and Irene and Nor'easters during early November and December during SHOWEX, and Hurricane Ivan during SAX 04. During SHOWEX, the rms wave heights reached 5.3 m during Hurricane Floyd, and 3.3 m during Hurricane Irene. During SAX 04, the rms wave heights reached 5.2 m during Hurricane Ivan, and further offshore rms wave heights of up to 10 m were noted (Fernandes, 2005).

Time series of rms wave heights at all sites are shown in Figure 13. Note that the vertical scale on the DUCK 94 plot differs from the scale used for SHOWEX and SAX 04. All of the hurricanes that passed near to the experimentation area are annotated on the figure. There were also times when nor'easters passed through the area, but these storms are not annotated on the figure.

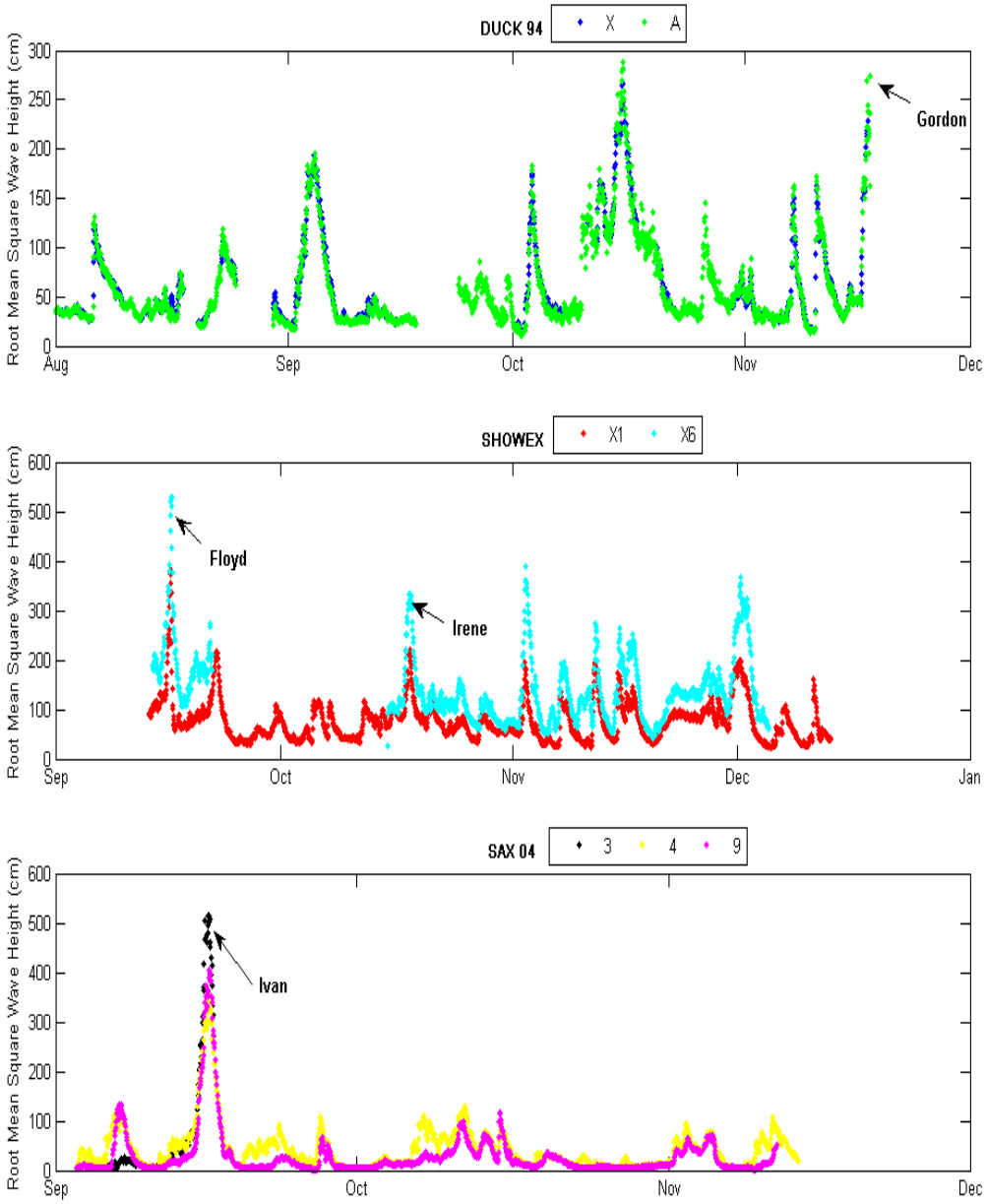

Figure 13. H_{rms} for all experiments with hurricanes annotated.

Before examining the sea-state dependence of wave height statistics, it is useful to create an averaged histogram for each sensor to verify if the Rayleigh distribution is a good overall fit to the averaged wave height distribution. An average histogram was formed for a given site by averaging the normalized relative frequency counts of the hourly histograms for each bin. In Figure 14 the average histograms of wave heights at each site generated from all the sea surface height data collected at that site are compared

with the Rayleigh pdf. These histograms, much like those presented in Thornton and Guza's study (Figure 7), show that the distribution of wave heights at all sites agree very closely with the Rayleigh distribution.

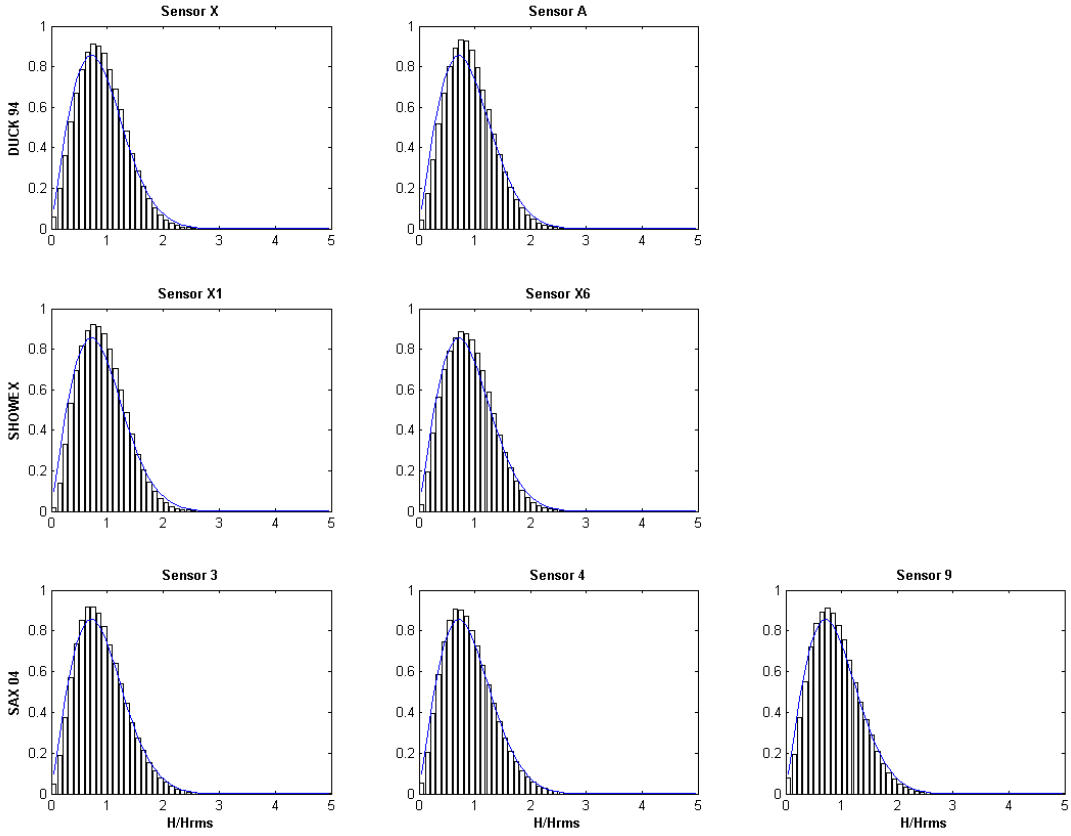

Figure 14. Averaged histogram at each site. The blue curve indicates the Rayleigh pdf.

Table 2. Number of total waves and extreme waves recorded for the seven sensors used from the three ONR sponsored experiments.

EXPERIMENT	SITE IDENTIFIER	TOTAL WAVES RECORDED	EXTREME WAVES RECORDED
DUCK 94	X	423719	32
DUCK 94	A	971659	152
SHOWEX	X1	1468075	116
SHOWEX	X6	822243	79
SAX 04	3	971595	306
SAX 04	4	1105962	383
SAX 04	9	154245	44

2. Wave Statistics Dependence on Sea State and Water Depth

Previous research has noted the important effect of nonlinearity on wave height statistics. Generally, nonlinearity does not effect the wave height distribution in lower energy sea states; it only has an appreciable effect in higher sea states. In this section, the data are categorized into low and high energy levels and the histograms are averaged in these categories to see if a nonlinear effect is noticeable in the observed statistics.

A threshold of two meters was selected as the root mean square wave height at which the sea state is characterized as "high energy." The threshold was chosen to be high enough to identify records with possible strong nonlinearity in the tail of the distribution, but low enough so there are sufficient data points in the high energy averaged histogram to make the evaluation of extreme wave occurrences statistically significant. Since a histogram was generated for each hour from all of the data sets, the normalization previously conducted allowed the averaging of histograms of similar sea states for comparison.

High energy time periods were defined as times when H_{rms} was greater than the threshold. Low energy time periods were defined as times when H_{rms} was between 0.5 m and 1 m. The definition of "low energy" was chosen so the averaged histogram would not be contaminated by wave conditions that approach the high energy threshold. Cases with rms wave heights below 0.5 m were excluded since these records may be degraded by too low of a signal to noise ratio.

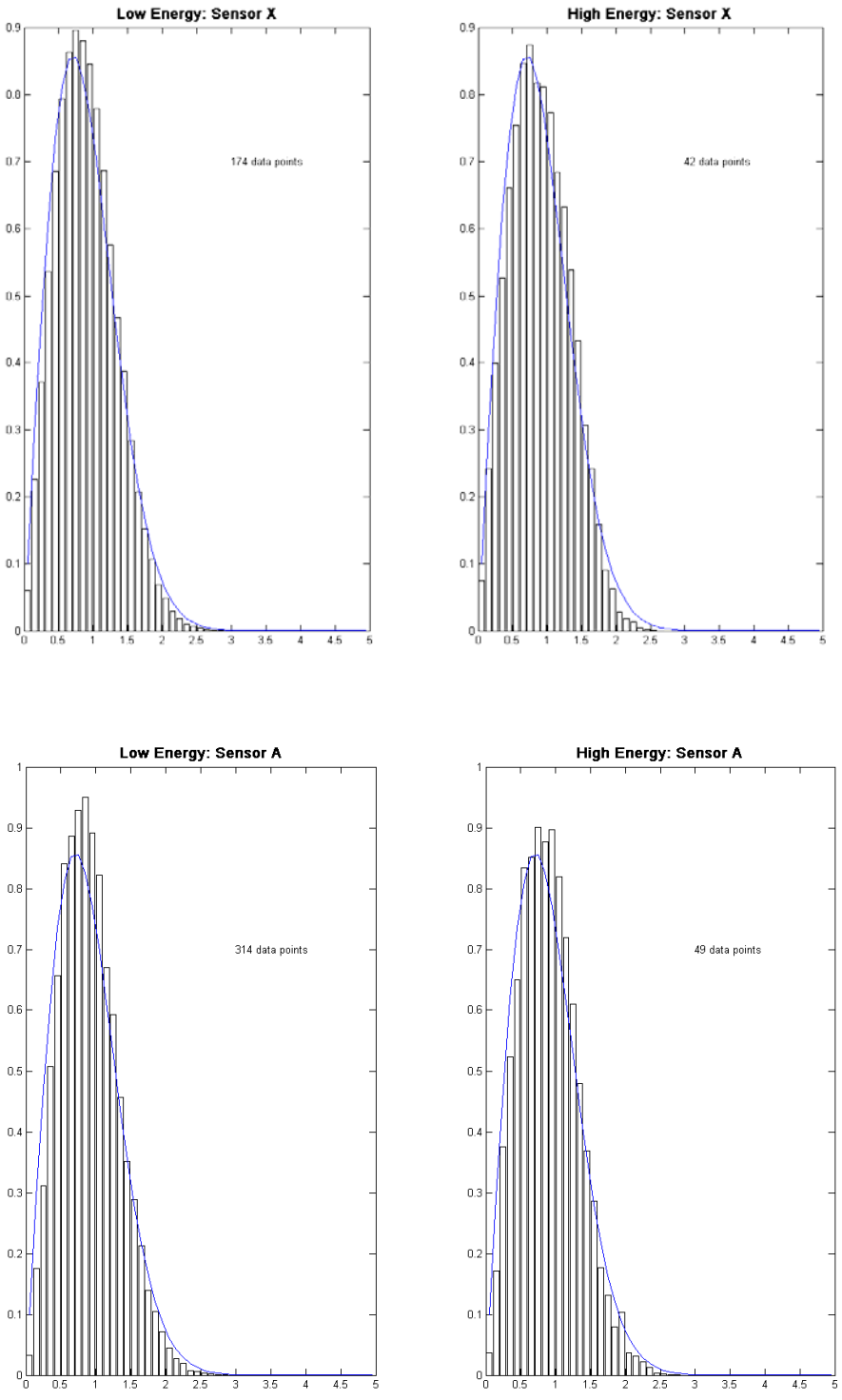

Figure 15. Averaged histograms for the DUCK 94 experiment. Left panels: low energy conditions, Right panels: high energy conditions.

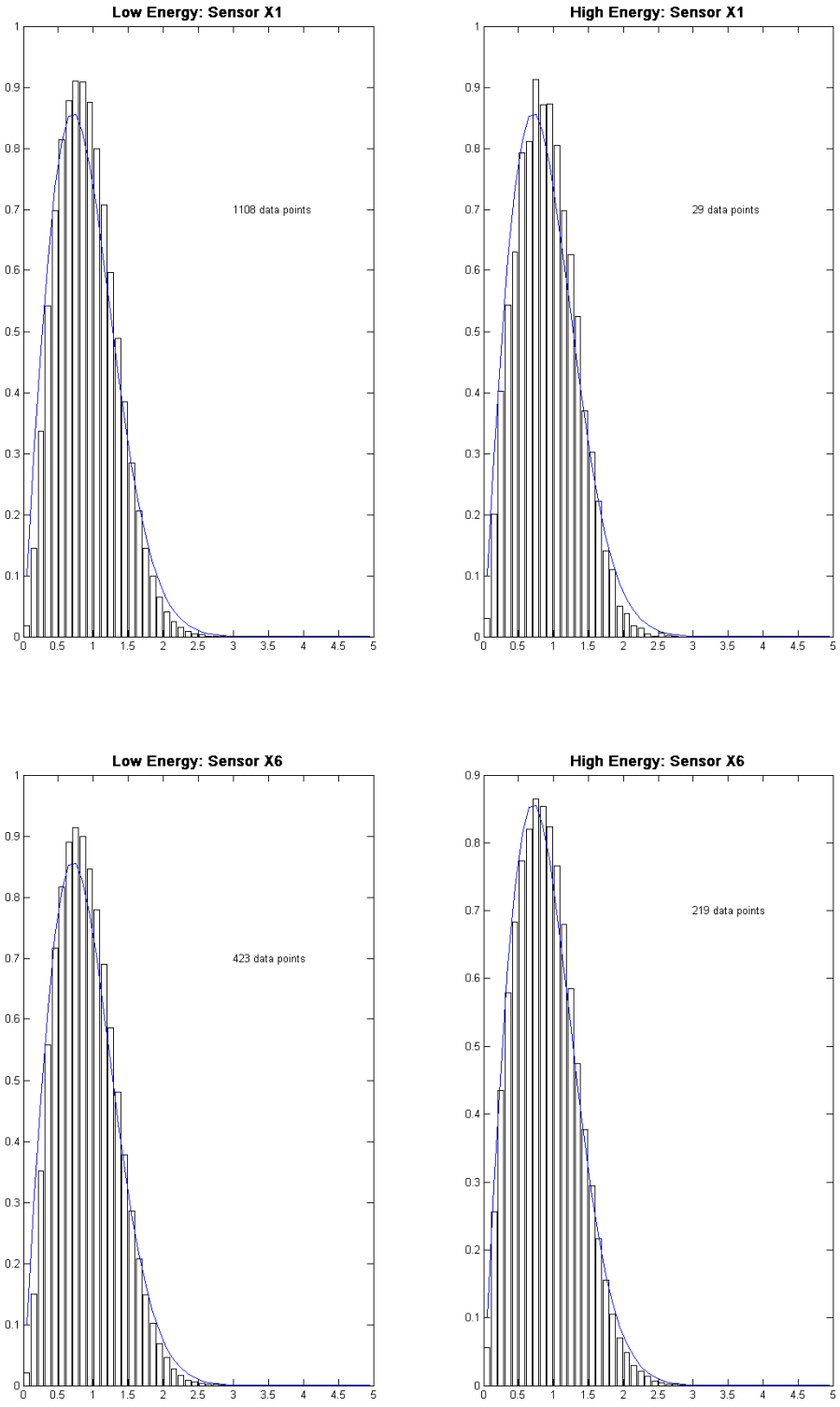

Figure 16. Averaged histograms for the SHOWEX experiment. Left panels: low energy conditions, Right panels: high energy conditions.

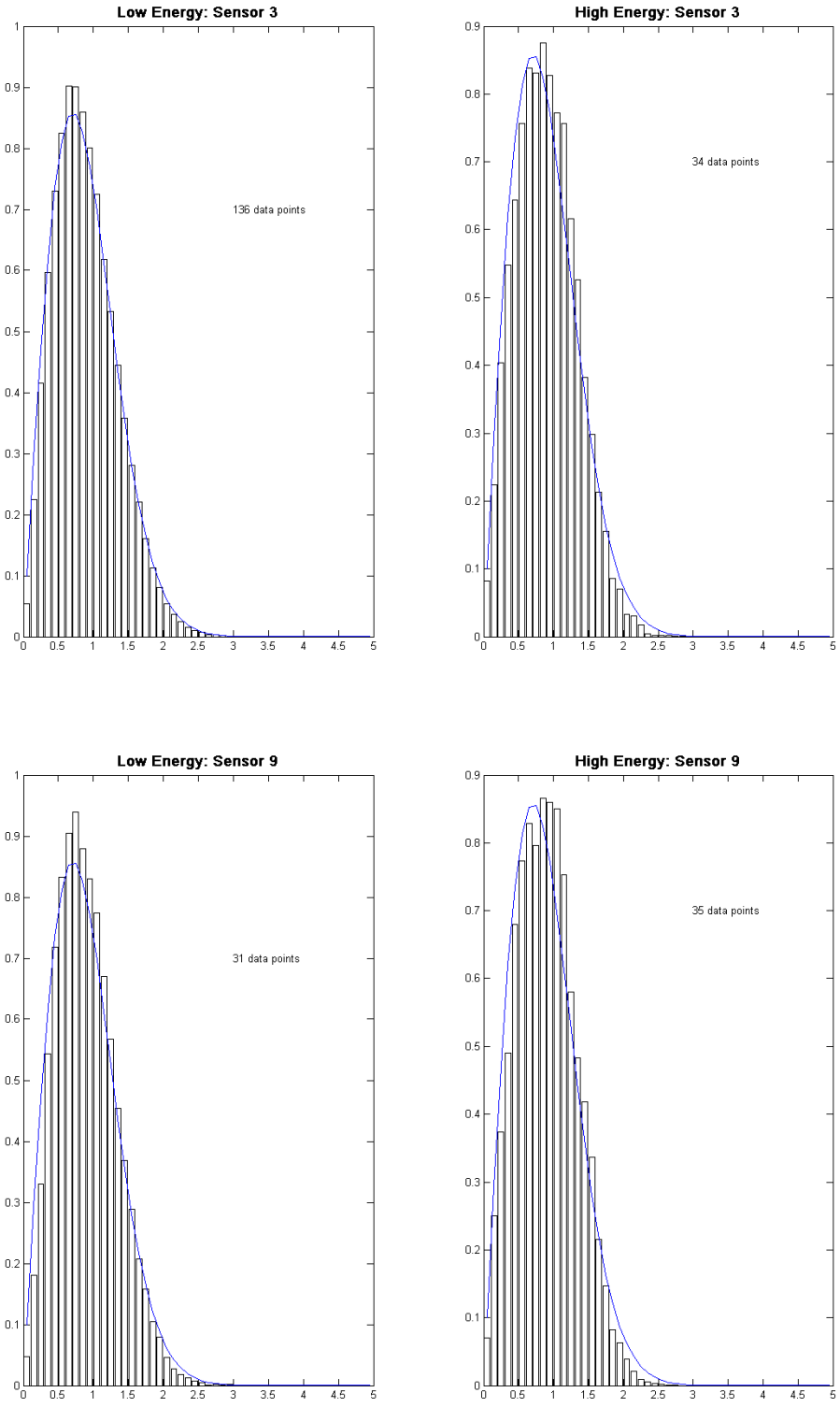

Figure 17. Averaged histograms for the SAX 04 experiment. Left panels: low energy conditions, Right panels: high energy conditions.

Figures 15-17 show the averaged histograms for low energy sea states (left panels, 0.5 m $< H_{rms} <$ 1 m) and high energy sea states (right panels, $H_{rms} >$ 2 m). Examining the averaged histograms from the DUCK 94 experiment (Figure 15), it can be observed that in benign sea states the wave statistics of both Sensor X and A are described well using the Rayleigh distribution. However, at site X there is a significant deviation from the Rayleigh distribution in the right-hand tail in the high energy histogram. The effect is less significant at Sensor A. There could be a few effects that explain this difference in deviation from the Rayleigh distribution. One explanation is that Sensor X was in the surf zone and the breaking and dissipation of larger waves may be the cause of the deviation. Another possibility is that the effects of nonlinearity played a stronger role in distorting the wave height distribution at the shallower sensor X as compared to the deeper sensor A during excited sea states.

The averaged histograms from SHOWEX (Figure 16) show a similar difference between the results at Sensors X1 and X6. The averaged high energy histogram from the shallow water Sensor X1 again shows a deviation in the right-hand tail of the wave height distribution from Rayleigh, much like that of Sensor X from the DUCK 94 experiment. However, the deep water site X6 does not show a similar deviation. In fact, at this sensor the high energy histogram follows Rayleigh just as well as the low energy histogram.

From the SAX 04 experiment, the averaged histograms categorized by sea state (Figure 17) show the same effect of a deviation in the right-hand tail in the high energy case. One point of interest is that both Sensors 3 and 9 were in shallow water separated alongshore by about 110 km. While the recorded waves were statistically independent from each other due to the geographic distance between them, the averaged histograms are similar, confirming that the deviations from the Rayleigh pdf are statistically significant.

3. Extreme Wave Height Statistics

During SHOWEX and SAX 04, there were three hurricanes which generated rms wave heights larger than 3 m. To investigate the statistics of these extreme waves, average histograms of wave records with H_{rms} exceeding 3 m are shown in Figure 18. Results are shown for shallow water sensor 9 in SAX 04 and deep water sensor X6 in

SHOWEX. The histograms are similar to the ones obtained at the same sites using the lower 2 m threshold, indicating that the analysis is not overly sensitive to threshold choice.

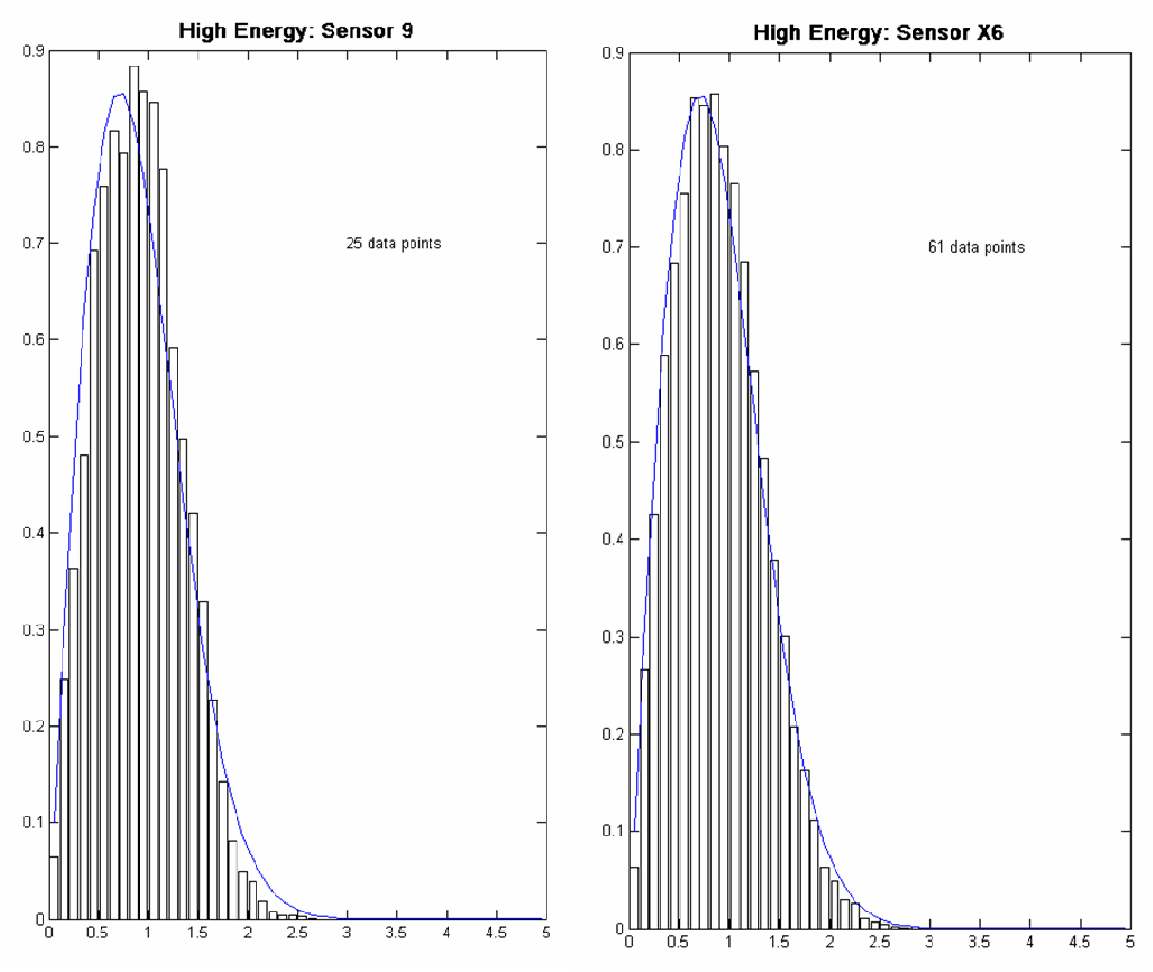

Figure 18. Averaged histograms from hours with a H_{rms} greater than 3 m.

The averaged histogram from the shallow water site (Sensor 9, shown in the left panel of Figure 18) shows a systematic deviation from the Rayleigh distribution with lower probabilities of large wave heights, similar to that obtained for the larger sample of waves exceeding 2 m rms wave height (lower right hand panel in Figure 17). Similarly, the averaged histogram from the deep water site (Sensor X6, shown in the right panel of Figure 18) follows the Rayleigh distribution very well, much like the lower right hand panel in Figure 16. So this distortion of the histograms in shallow water

that is not observed in deep water is a robust feature of these data sets that is insensitive to the choice of the wave height threshold.

B. CASE STUDIES OF EXTREME WAVES

In this section, the analysis moves from an overall statistical overview of the data, to describing short time series of the sea surface height, primarily during hurricanes. Time series were selected with one or more waves whose height is at least twice as large as the significant wave height (2.8 times the rms wave height). The objective of this analysis is to examine the characteristics of these so-called freak waves.

1. Extreme Waves Found During and Following Extreme Events

a. Hurricane Floyd, Site X6

The first case study was taken from the SHOWEX experiment. On September 16, 1999, Hurricane Floyd passed through the experiment area, and generated high energy waves. The time series shown in Figure 19 was taken from the hour during Hurricane Floyd with the largest H_{rms}. The two waves annotated with red lines were the largest waves that were found at Site X6.

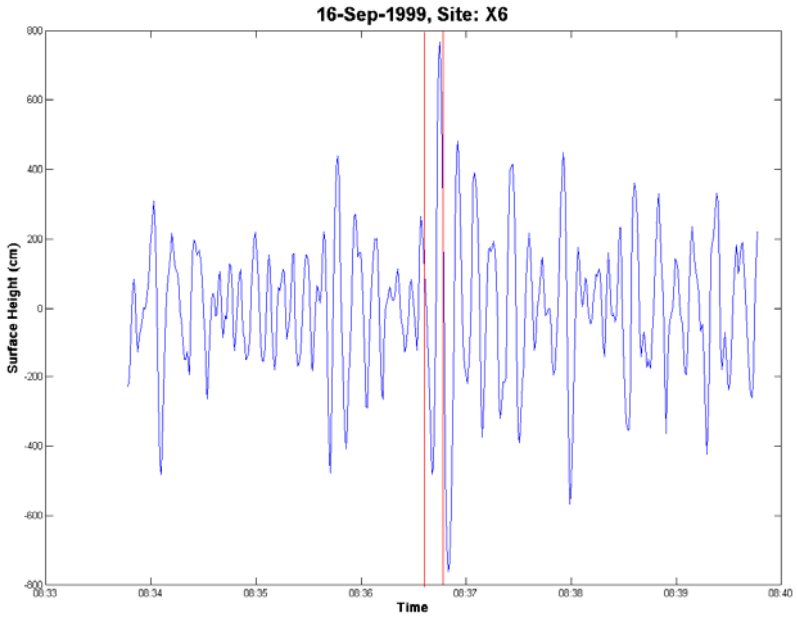

Figure 19. Extreme Waves from SHOWEX, Hurricane Floyd, Site X6. The extreme waves are annotated with red lines that indicate the beginning of the wave as the sea surface crosses zero in the downward direction.

The root mean square wave height for the entire hour record was 4.91 m. Note that the second wave has a deep trough following a large crest from the first extreme wave; the total drop from the crest of the first wave to the trough of the second wave is almost 16 m. This time series agrees well with the qualitative reports from mariners that when they encountered a freak wave it felt as if their vessel fell into a "hole in the ocean." Also note that the two waves preceding the two freak waves are much smaller than the rest of the waves in this six minute time series. This behavior could be indicative of the nonlinear instability mechanism discussed by Trulsen (1999) in his study of rogue waves (Figure 5). It is interesting to note in this case that if a zero up-crossing analysis was used instead of a zero down-crossing method, the extreme waves shown in Figure 19 would register a 16 m drop from crest to trough.

b. Hurricane Floyd, Site X1

The second case study selected for further examination is from the same one-hour time period during Hurricane Floyd, but from Site X1 that was in a much shallower depth (21 m) as compared to Site X6 (195 m). The root mean square wave height was also lower at X1 (3.74 m as compared to 4.91 m at Site X6), possibly because some of the wave energy was lost due to bottom friction or enhanced wave breaking in shallow water. Again, this time series was selected because it was the most energetic wave record collected at Site X1, and the wave annotated in Figure 20 is the highest wave in the record.

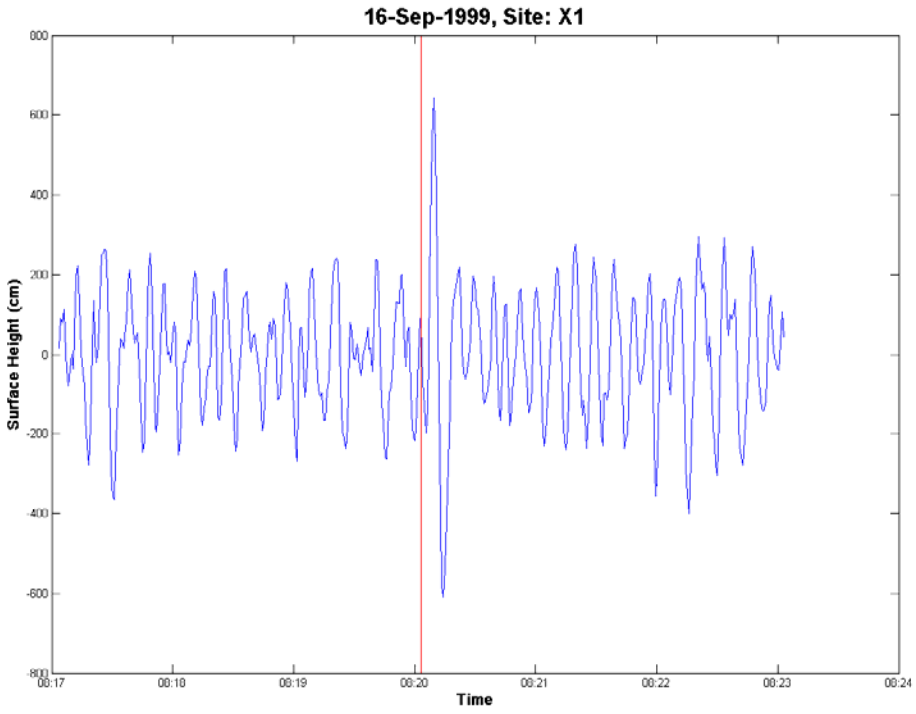

Figure 20. Extreme Wave from SHOWEX, Hurricane Floyd, Site X1 (same format as Figure 19).

This case is interesting in that it shows a single isolated large wave in a fairly uniform background. As in the previous example a deep trough follows the high crest. This extreme wave looks much like the New Year Wave measured at the Draupner platform (Figure 2), just on a smaller scale. The New Year Wave had an amplitude of 18.5 m, which was more than three times the average wave amplitude for that wave train. Here during Hurricane Floyd, the average wave amplitude was approximately 2 m and the amplitude of the extreme wave shown in Figure 20 was 6.2 m. Much like Figure 19, if a zero up-crossing method was applied to the waves in Figure 20, the drop from the crest to the trough is over 12 m!

c. Hurricane Irene, Site X6

Another extreme event in the SHOWEX data set is Hurricane Irene. The time series shown in Figure 21 was taken from the hour during Hurricane Irene with the largest H_{rms} (H_{rms}=3.34 m). The annotated extreme wave was the largest wave during Hurricane Irene found in the wave record from Site X6.

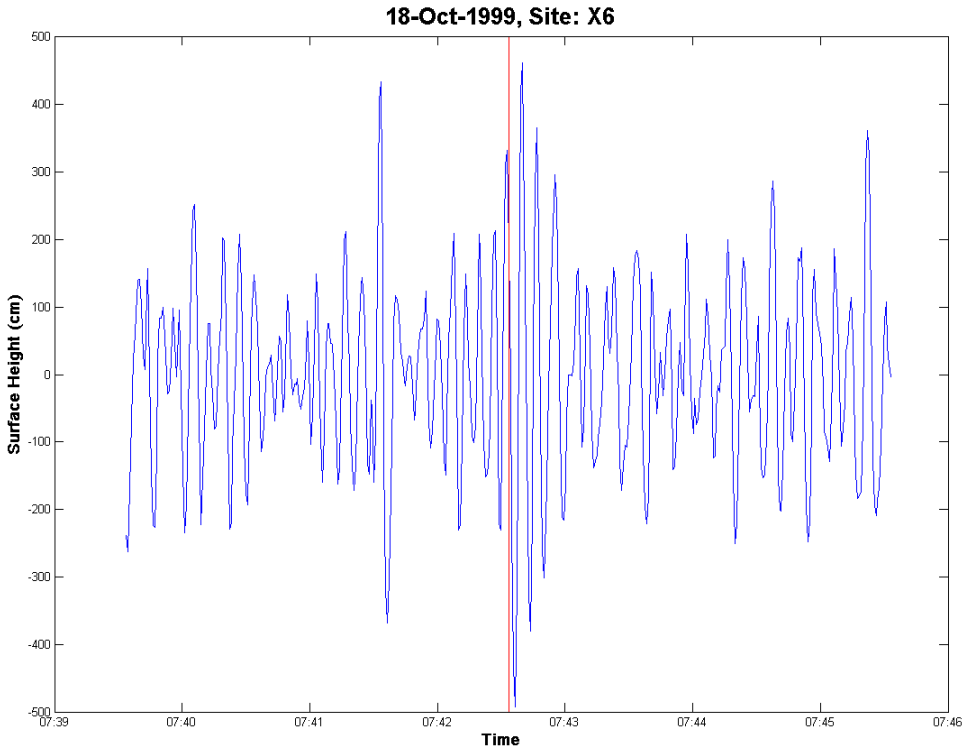

Figure 21. Extreme Wave from SHOWEX, Hurricane Irene, Site X6 (same format as Figure 19).

The extreme wave in Figure 21 (or the large wave arriving a minute earlier in Figure 21) does not show the same isolated structure as the previous case studies. Instead, the extreme wave is part of a group of large waves with the maximum amplitude near the center of the group. The wave groups do seem to become rather disorganized after the extreme wave. It is not until several minutes later (not shown in Figure 21) that the 'groupiness' property of the time series returns.

d. After Hurricane Irene, Site X1

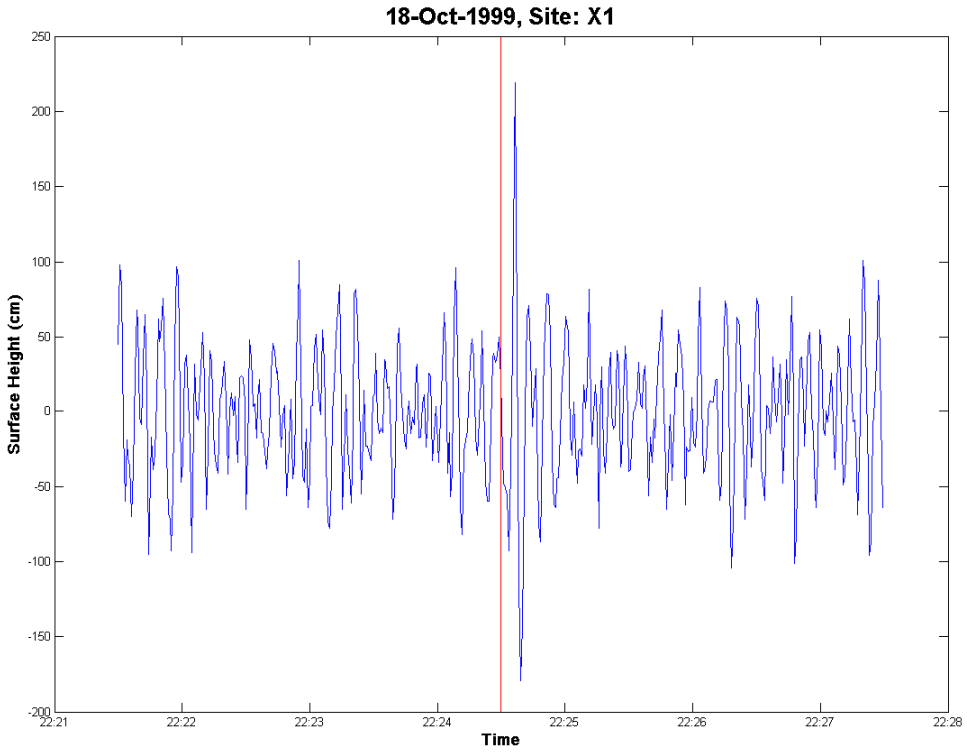

Figure 22. Extreme Wave from SHOWEX, After Hurricane Irene, Site X1 (same format as Figure 19).

Unlike the three previous case studies this SHOWEX case was obtained in relatively benign conditions (H_{rms}=1.1 m) after Hurricane Irene passed through the area. Again the extreme wave's high crest is followed by a deep trough and the local crest to trough excursion is much larger than the surrounding waves, even in a relatively benign sea state. This feature of Figure 22 has important naval operational applications. Small boat or amphibious operations could be conducted in wave conditions with a root mean square wave height of 1.1 m (or a significant wave height of 1.55 m) but if those units encountered an unexpected 4 m wave like that shown in Figure 22, major equipment damage could occur. Therefore, units conducting small boat or amphibious operations should be aware that even in relatively benign wave conditions, they take on the risk of encountering an isolated large wave that may damage equipment or jeopardize safety of personnel.

2. Shoaling Transformation During Extreme Events

In this section, longer time series are examined during hurricanes to investigate the changes in wave characteristics as they propagate from a deeper water site to a shallower site.

a. Hurricane Ivan, From Deep Water (Site 7) to Intermediate Depth (Site 9)

Sea surface height time series from Hurricane Ivan estimated from a deep water site (Site 7 is in 85 m depth) is shown in the top panel of Figure 23 and from an intermediate depth site (Site 9 is in 18 m depth) in the bottom panel of Figure 23. Each time series shown is 30 minutes long. In order to compare approximately the same waves, there is a 40 minute offset between the time series to allow for travel time (i.e., distance/group speed) of the waves from one site to the other. This travel time was calculated based on the peak period and average water depth between the two sites. Owing to the large depth at site 7, only waves with periods longer than about 10 s can be measured reliably with a seafloor pressure sensor. Therefore a low-pass filter with a frequency cutoff of 0.1 Hz was applied to the wave records at both sites 7 and 9 so that the time series contain only the dominant part of the spectrum.

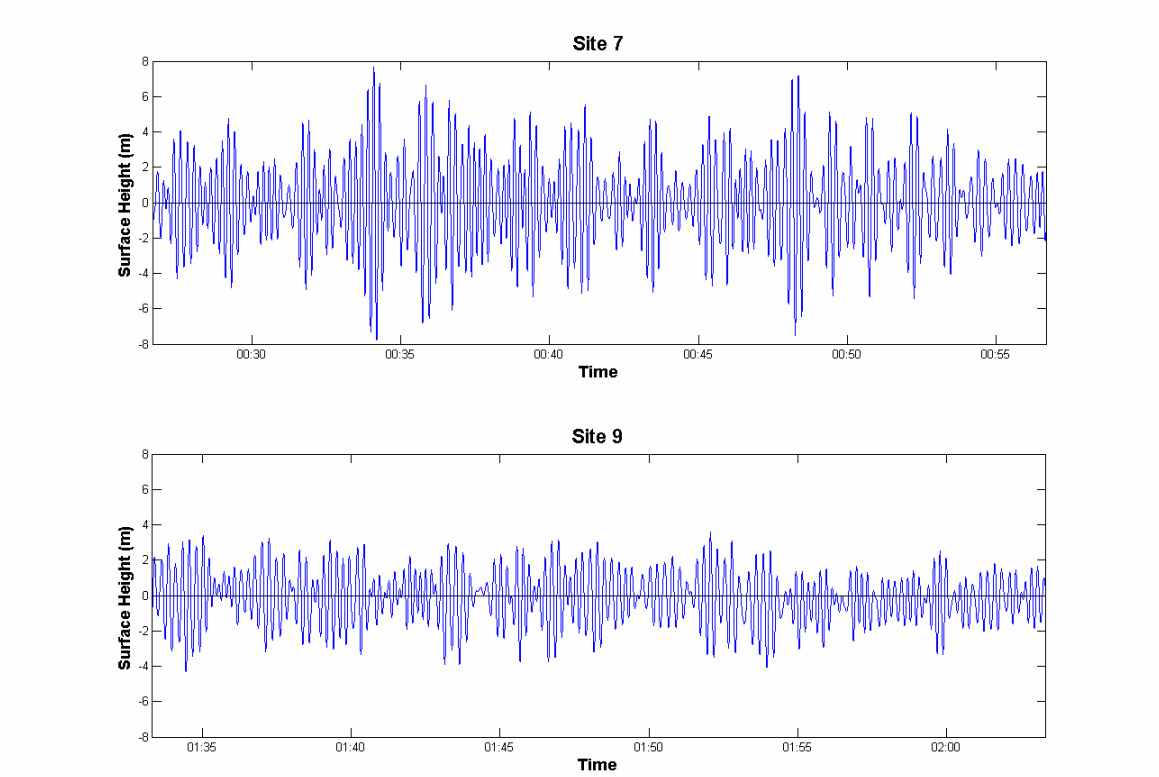

Figure 23. Shoaling Transformation during Hurricane Ivan, 16 September 2004, from a deep water site to an intermediate depth site.

As the waves travel from Site 7 to Site 9, they become more uniform in height. This behavior agrees with what was observed in the histograms (Figure 18, left panel). A possible explanation for this behavior could be that nonlinear instability, which can produce large waves in deep water, is suppressed in shallow water (Janssen, 2003).

b. Hurricane Gordon, From Intermediate Depth (Site A) to Shallow Water (Site X)

The next time series is obtained from the DUCK 94 experiment in the lead up to Hurricane Gordon. As was noted earlier, both Sensors A and X failed during the hurricane due to being buried by sand. Sensor A was in 12 m depth, located just outside the surf zone, and Sensor X was in 6 m depth, in the surf zone. This section examines the differences in the wave groups as well as the structure of the waves as they propagate from Sensor A to Sensor X. These two sites are separated by only a distance of 1 km, so there is a much shorter propagation time delay (about 2 minutes) between the time series than in the previous example from Hurricane Ivan.

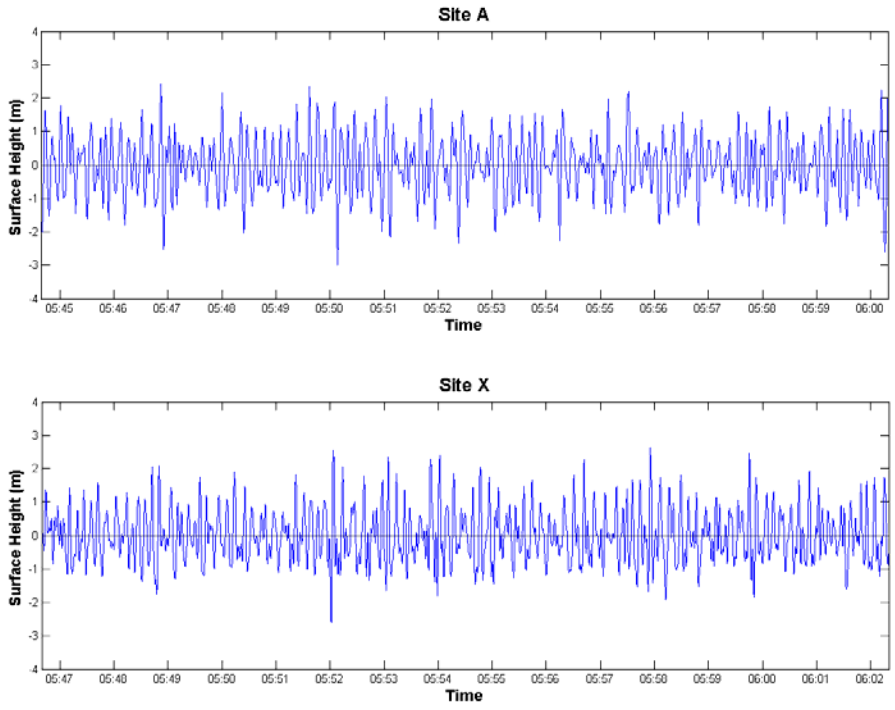

Figure 24. Shoaling transformation during the lead up to Hurricane Gordon, 17 November 1994, from an intermediate depth site (Sensor A, 12 m) to a shallow site (Sensor X, 6 m). The time series are offset by two minutes to account for the propagation delay between the two sites.

Note in Figure 24 that the wave heights at Site A are already fairly homogeneous in nature. There is not a drastic change in the group structure from the deeper to the shallow site like was noted in the example from Hurricane Ivan. The time series from Site A (top panel of Figure 24) looks similar to the time series from the intermediate depth site from the SAX 04 data (bottom panel of Figure 23). What is interesting to note, however, is how the structure of the waves change as they cross through the surf zone. A time series of 4 minutes in length was extracted from the plot displayed in Figure 24, and re-plotted in Figure 25 to more closely examine the changes in the shape of the waves.

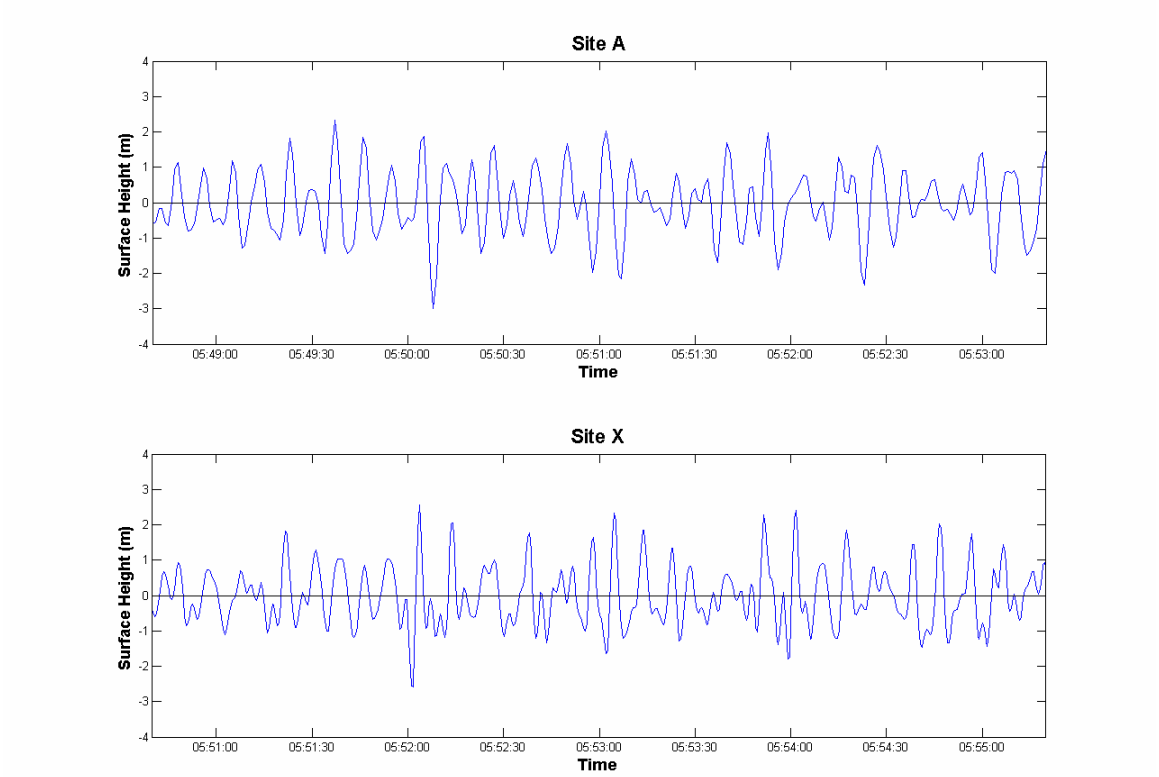

Figure 25. Shoaling transformation during the lead up to Hurricane Gordon, 17 November 1994, from an intermediate depth site to a shallow site. A 4 minute record is shown in order to more closely examine the structure of the waves as they cross into the surf zone.

The waves observed at Site A are more symmetrical as compared to the waves from Site X. This is in agreement with findings from previous studies concerning shoaling transformation across a surf zone (Elgar and Guza, 1985). As the waves propagate from Site A to Site X across the surf zone, they become more nonlinear in shape. The waves from Site X have a noticeable sawtooth property, that is, the front side of the wave has a very steep slope, and the back side of the wave is more gradual. This shoaling transformation has important applications for naval small boat operations since the steep, nearly breaking, waves at the shallower site (Sensor X) pose a greater hazard to equipment and personnel than the nearly sinusoidal waves of similar height observed only 1 km seaward (Sensor A).

V. CONCLUSIONS AND FUTURE RESEARCH

This thesis examines observed statistics of wave heights and the occurrence of freak waves in coastal regions using data from the ONR-sponsored DUCK 94, SHOWEX and SAX 04 experiments. Previous observations of freak waves were mostly limited to deep water regions; very little research has been conducted concerning the characteristics of these waves in coastal areas. This study compares statistics from energetic wave fields across several depths of water to more comprehensively understand the frequency of occurrence and nature of extreme waves as they propagate from the open ocean toward shallow coastal areas where naval forces generally operate.

This study is consistent with previous research in its finding that wave height distributions in both shallow and deep water regions generally follow the theoretical Rayleigh distribution for a linear narrow band wave field. Even in high energy sea states, there are not many extreme waves present; most of the waves fall well within the Rayleigh distribution. Although on average the wave height statistics agree well with the Rayleigh model, significant differences are observed between high and low energy sea states and between deep and shallow water sites. During high-energy events, such as hurricanes, the shallow sites show fewer extreme waves than during low-energy conditions; their wave height distributions become narrower as hurricanes or storms pass over the experimentation area. Deep water sites, on the other hand, show relatively the same number of extreme waves whether the sea state is high-energy or low energy. That is, deep water sites follow the Rayleigh distribution well in all sea states, but shallow water sites show a significant deviation in the right-hand tail of the distribution of wave heights from Rayleigh during high-energy events.

Additionally, this study has validated previous studies findings of shoaling transformation from deeper water to shallower water. In extreme events, waves become more homogeneous and lose their group structure as they propagate into shallower water. This finding is consistent with the averaged histograms of wave heights in high energy conditions that are notably narrower at the shallower sites. As waves propagate into very shallow water across the surf zone, the characteristics of the wave groups do not change

much, but the properties of the individual waves do change. Outside the surf zone, the waves are symmetrical in shape, but after they pass through the surf zone, they become asymmetrical and saw-tooth shaped.

This research topic has important implications for commanders' risk management practices when planning nearshore naval operations. Just because most of the observed extreme waves fell neatly into the Rayleigh distribution does not mitigate their destructive power if a small craft should encounter one. This study did find a few very large waves as compared to the surrounding waves during times of relatively low-energy sea states. If a small craft would encounter one of these waves, major equipment damage could occur, not to mention, placing the personnel within the craft in peril. A commander must determine what level of risk is acceptable, and this study demonstrates that even during low-energy sea states there is a risk of encountering an isolated so-called freak wave. Instead of relying solely on average wave parameters (e.g., significant wave height, peak period), distributions such as those presented in this thesis are needed for risk assessment. Additionally, the development of new real-time wave monitoring capabilities on ships (e.g., shipboard radar) coupled with numerical models should be explored for greater awareness of the wave environment during Navy operations.

Since the Indian Ocean tsunami on December 26, 2004, much attention has been focused on developing pressure sensor networks to give earlier warnings. Due to the great depths that these sensors are placed at, they are unsuitable for obtaining sea surface elevation time series. The deep water column between the sea surface and these pressure sensors prevent recovery of high frequency wind-generated waves. The National Data Buoy Center (NDBC) has wave monitoring networks of wave buoys, but they only collect spectral data, not sea surface elevation time series. To expand this research on extreme waves to include more data sets, current sensor networks would need to be augmented by sensors whose primary purpose is the collection of sea surface elevation time series.

There are several avenues for further in-depth study of freak waves. This study was solely based on wave height statistics; other possibilities include study of characteristics such as the steepness or shape of individual freak waves. Further research

could be conducted by examining the group structure of freak waves to determine if they are more likely to be found in groups of multiple large waves or whether they tend to be more isolated in nature. Much of the up and coming research concerning freak waves deals with studying their presence within numerical models. Currently, researchers are developing 3D models of the ocean surface, and as these come online, realistic simulations of freak waves in the battlespace environment will be possible.

THIS PAGE INTENTIONALLY LEFT BLANK

LIST OF REFERENCES

Ardhuin, F., O'Reilly, W. C., Herbers, T. H. C., & Jessen, P. F. (2003). Swell Transformation across the Continental Shelf. Part I: Attenuation and Directional Broadening. *Journal of Physical Oceanography, vol. 33,* 1921-1939.

Draper, L. (1964). 'Freak' Ocean Waves. *Oceanus, vol. 4,* 12-15.

———. (1971). Severe Wave Conditions at Sea. *Journal of the Institute of Navigation, vol. 24, no. 3,* 273-277.

Dysthe, K. B. (2000). Modeling a "Rogue Wave" – Speculations or a Realistic Possibility? In *Rogue Waves 2000,* Brest, France, 2000.

——— Krogstad, H., Socquet-Juglard, H. & Trulsen, K. (January 2006) Freak waves, rogue waves, extreme waves and ocean wave climate. Retrieved February 16, 2006, from http://www.math.uio.no/~karstent/waves/index_en.html.

——— & Trulsen, K. (1999). Note on breather type solutions of the nonlinear Schrödinger equation as models for freak-waves. *Physica Scripta vol. T82,* 48-52.

Elgar, S. & Guza, R. T. (1985). Observations of bispectra of shoaling surface gravity waves. *J. Fluid Mech., vol. 161,* 425-448.

Fernandes, C. A., (2005). Extreme Hurricane Generated Waves in the Gulf of Mexico. Master's Thesis, Naval Postgraduate School, Monterey, California.

Herbers, T. H. C., Hendrickson, E. J., & O'Reilly, W. C. (2000). Propagation of swell across a wide continental shelf. *Journal of Geophysical Research vol. 105, no. c8,* 19729-19737.

Haver, S. (2000a). A Possible Freak Wave Event Measured at the Draupner Jacket January 1 1995. Retrieved May, 4, 2006, from http://www.ifremer.fr/web-com/stw2004/rw/fullpapers/walk_on_haver.pdf.

———. (2000b). Some Evidences of the Existence of So called Freak Waves. In *Rogue Waves 2000,* Brest, France, 2000.

Janssen, P. A. E. M. (2003). Nonlinear Four-Wave Interactions and Freak Waves. .*Journal of Physical Oceanography, vol. 33,* 863-884.

Lawton, G. (2001). Monsters of the Deep. *New Scientist, vol. 170,* 28.

Longuet-Higgins, M. S. (1952). On the statistical distribution of the heights of sea waves, *J. Mar. Res.., vol. 11(3),* 245-266.

Osborne, A., Onorato, M. & Serio, M. (2000). The nonlinear dynamics of rogue waves and holes in deep water gravity wave trains. *Phys. Lett. A, vol. 275,* 386-393.

Pelinovsky, E., Kharif, C., Talipova, T. & Slunyaev, A. (2000). Nonlinear Wave Focusing as a Mechanism of the Freak Wave Generation in the Ocean. In *Rogue Waves 2000,* Brest, France, 2000.

Rosenthal, W. (2006). Freak Waves: Tracking down the secret of the giant waves. Retrieved May, 3, 2006, from http://www.helmholtz.de/en/Research_Fields/Transport_and_Space/INSIGHT.html.

Thornton, E. B. & Guza, R. T. (1983). Transformation of Wave Height Distribution, *Journal of Geophysical Research, vol. 88, no. c10,* 5925-5938.

Tinder, C. V., (2000). Swell Transformation Across the Continental Shelf. Master's Thesis, Naval Postgraduate School, Monterey, California.

Trulsen, K. B., (1999). Wave kinematics computed with the nonlinear Schrödinger method for deep water. *J. Offshore Mechanics and Arctic Engineering* vol. *121(2)*,126-130.

——— Gudmestad O. T. & Velarde M. T. (2001) The nonlinear Schrödinger method for water wave kinematics on finite depth. *Wave Motion* vol. *33*, 379-395.

White, B. S. & Fornberg, B. (1998) On the Chance of Freak Waves at Sea. *J. Fluid Mech. vol. 355*, 113-138.

INITIAL DISTRIBUTION LIST

1. Defense Technical Information Center
   Ft. Belvoir, Virginia

2. Dudley Knox Library
   Naval Postgraduate School
   Monterey, California

3. Professor Mary L. Batteen
   Department of Oceanography
   Naval Postgraduate School
   Monterey, California

4. Professor Thomas H. C. Herbers
   Department of Oceanography
   Naval Postgraduate School
   Monterey, California

5. Professor Edward B. Thornton
   Department of Oceanography
   Naval Postgraduate School
   Monterey, California

6. Mr. Paul Jessen
   Department of Oceanography
   Naval Postgraduate School
   Monterey, California